3-12-2020

# Incorporation of Agouti-Related Protein (AgRP) Human Single Nucleotide Polymorphisms (SNPs) in the AgRP-Derived Macrocyclic Scaffold c[Pro-Arg-Phe-Phe-Asn-Ala-Phe-dPro] Decreases Melanocortin-4 Receptor Antagonist Potency and Results in the Discovery of Melanocortin-5 Receptor Antagonists

Zoe M. Koerperich
*University of Minnesota*

Mark D. Ericson
*University of Minnesota*

Katie T. Freeman
*University of Minnesota*

Robert C. Speth
*Nova Southeastern University; Georgetown University*, rs1251@nova.edu

Irina D. Pogozheva
*University of Michigan*

*See next page for additional authors*

Published in final edited form as:

*J Med Chem*. 2020 March 12; 63(5): 2194–2208. doi:10.1021/acs.jmedchem.9b00860.

# Incorporation of Agouti-Related Protein (AgRP) Human Single Nucleotide Polymorphisms (SNPs) in the AGRP-Derived Macrocyclic Scaffold c[Pro-Arg-Phe-Phe-Asn-Ala-Phe-DPro] Decreases Melanocortin-4 Receptor Antagonist Potency and Results in the Discovery of Melanocortin-5 Receptor Antagonists

**Zoe M. Koerperich**[1], **Mark D. Ericson**[1], **Katie T. Freeman**[1], **Robert C. Speth**[2,3], **Irina D. Pogozheva**[4], **Henry I. Mosberg**[4], **Carrie Haskell-Luevano**[1,*]

[1]Department of Medicinal Chemistry and Institute for Translational Neuroscience, University of Minnesota, Minneapolis, MN 55455 USA

[2]College of Pharmacy, Nova Southeastern University, Fort Lauderdale, Florida 33328-2018, United States

[3]College of Medicine, Georgetown University, Washington, D.C. 20057, United States

[4]Department of Medicinal Chemistry, University of Michigan, Ann Arbor, MI 48109 USA

## Abstract

While the melanocortin receptors (MCRs) are known to be involved in numerous biological pathways, the potential roles of the MC5R have not been clearly elucidated in humans. AgRP, an MC3R/MC4R antagonist and MC4R inverse agonist, contains an exposed ß-hairpin loop composed of six residues (Arg-Phe-Phe-Asn-Ala-Phe) that is imperative for binding and function. Within this active-loop of AgRP, four human missense polymorphisms were deposited into the NIH Variation Viewer database. These polymorphisms, Arg111Cys, Arg111His, Phe112Tyr, and Ala115Val (AgRP full-length numbering) were incorporated into the peptide macrocycles c[Pro$^1$-Arg$^2$-Phe$^3$-Phe$^4$-Xaa$^5$-Ala$^6$-Phe$^7$-DPro$^8$], where Xaa was Dap$^5$ or Asn$^5$, to explore the functional effects of these naturally-occurring substitutions in a simplified AgRP scaffold. All peptides lowered potency at least 10-fold in a cAMP accumulation assay compared to the parent sequences at the MC4Rs. Compounds MDE 6-82-3c, ZMK 2-82, MDE 6-82-1c, ZMK 2-85, and ZMK 2-112 are also the first AgRP-based chemotypes that antagonize the MC5R.

*Corresponding author to whom reprint requests should be made. *Author Information*: Carrie Haskell-Luevano, Ph.D. Department of Medicinal Chemistry and Institute for Translational Neuroscience, University of Minnesota, 308 Harvard St SE, Minneapolis, Minnesota, 55455, United States; chaskell@umn.edu; Phone: 612-626-9262; Fax: 612-626-3114.

*Author Contribution*: Z.M.K., M.D.E. and C.H.-L. designed the experiments. Z.M.K. and K.T.F carried out the experiments. Z.M.K. analyzed the data with the assistance of M.D.E. and C.H.-L. I.D.P and H.I.M. modeled the ligands and the receptor. Radiolabeled compounds were prepared by R.C.S. Z.M.K. and C.H.-L. wrote the manuscript with contributions from other authors.

*Conflict of Interest*: The authors declare no conflict of interest.

Ancillary Information

*Supporting Information:* The supporting information is available free of charge and contains the analytical HPLC traces.

## Graphical Abstract

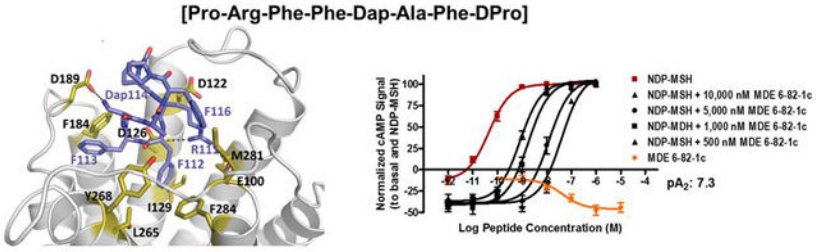


### Keywords

AGRP; macrocycles; melanocortin receptors; single nucleotide polymorphisms

## Introduction

Five unique melanocortin receptors (MCRs) have been identified to date.[1-8] These receptors are members of the family A of G protein-coupled receptors (GPCRs). The MCRs have been shown to be involved in several different physiological functions such as skin pigmentation (MC1R),[1,2] steroidogenesis (MC2R),[1,9] and energy homeostasis (MC3/4R).[10-13] While many biological activities have been attributed to the MC1–4Rs, the physiological role(s) of the MC5R have not been fully identified and characterized for this most ubiquitously expressed melanocortin receptor. Based upon the phenotype of the MC5RKO mice, the MC5R has been reported to be involved in sebaceous gland function.[14] The melanocortin receptor family is stimulated by several endogenous peptides including α-, ß-, and γ-melanocyte stimulating hormone (MSH) and adrenocorticotropin hormone (ACTH), all processed from the pro-opiomelanocortin (POMC) gene transcript.[15] In addition to these agonists, there are two known naturally occurring antagonists for the melanocortin receptor family: agouti-signaling protein (ASP)[16,17] and agouti-related protein (AgRP).[18,19] These antagonist peptides both contain an Arg-Phe-Phe motif in the carboxyl terminal region, as reviewed,[20] which has been proposed to be the sequence responsible for receptor affinity and antagonist activity.[21,22] AgRP is expressed centrally in the arcuate nucleus of the hypothalamus[19] and antagonizes the MC3R and MC4R,[4,19,23] effectively increasing feeding behavior.[13,24-26] Additionally, AgRP functions as an inverse agonist at the MC4R, decreasing the amount of cyclic adenosine monophosphate (cAMP) produced by the cell in the absence of the agonist ligand stimulation[27,28] Feeding studies reported that central administration of melanocortin agonists such as NDP-MSH (a synthetic potent analogue of α-MSH) or melanotan II (MTII, a potent cyclic analogue of α-MSH) decreased food intake and prevented weight gain in mice.[29-33] Contrarily, central injections of AgRP antagonist prompted long-acting increases in feeding behavior in fasted or sated animals.[19,32,34-36]

In addition to the reported activity of AgRP at the MC3R and MC4R, there have been mixed reports about AgRP at the MC5R. Pooled fractions of recombinant AgRP using a baculovirus expression system in insect cells resulted in a rightward potency shift of α-MSH in HEK293 cells expressing the hMC5R at 100 nM concentrations.[19] Another report using recombinant AGRP expressed from COS-7 cells indicated that AgRP was unable to displace

radiolabeled NDP-MSH at the hMC5R expressed in L cells at up to 40 nM concentrations, although functional activity was not determined.[18] A third report using chemically synthetized AgRP ligands [either the hAGRP(87-132) C-terminal domain, or a fusion of the mAGRP(21-85) to the hAGRP(87-132) generating the (Leu127Pro)AGRP] indicated that AgRP could functionally antagonize α-MSH at the MC5R at 100 nM concentrations, and could displace radiolabeled NDP-MSH ($IC_{50}$ = 310 nM) and radiolabeled AgRP ($IC_{50}$ = 26 nM) at the MC5R.[37] The differing reported activities could be due to the activity ranges assayed, varying degrees of AgRP purity based upon the methods used to generate the peptide, or cellular assay conditions between the different reports. Previous reports of AgRP derived ligands have not reported MC5R antagonist activity, although inverse agonist efficacy has previously been observed.[38,39]

Melanocortin ligands like MTII were originally developed before cloning of the receptors and to function as MC1R agonists in frog and lizard skin pigmentation assay. [30,40] After cloning of the receptors, these compounds were developed for the clinic to prompt melanogenesis (tanning of the skin), aide in melanoma detection, and as melanoma chemotherapeutics.[41-44] Since the early 2000's the MC4R, and to a lesser extent the MC3R, have been targeted due to their role in energy homeostasis and clinical indications in obesity and anorexia.[45-49] Obesity has grown to be an epidemic, with projections estimating that over 50% of Americans will be overweight or obese by 2030.[50] Approximately 5% of these cases are monogenic and linked to a disrupted central melanocortin system, where patients' obesity manifests in early childhood.[51-53] Diseases of negative energy imbalance, causing failure to thrive in young children, anorexia, and cachexia (disease-associated wasting) are also concerning because a decreased drive to eat can stunt growth in children and delay the body's response to healing.[47-49,54,55] Manipulation of the melanocortin system in either direction could offer a viable solution to combating these diseases and their associated comorbidities.

Activation of the MC4R leads to a decrease in food intake, but compounds that have made it into the clinic have ultimately failed due to unwanted side effects like increases in blood pressure,[56] darkening of the skin,[57,58] and increased erectile function,[59] as reviewed by Ericson *et al.* [60] One compound, RM-493 (Setmelanotide), manufactured by Rhythm Pharmaceuticals, has seen clinical success in obese patients that do not produce the POMC gene transcript by decreasing body weight without the increase in blood pressure seen in the clinic with other melanocortin compounds.[61] However, one patient with POMC deficiency was reported to have a decrease in diastolic blood pressure while being treated with RM-493 that was present during the extension phase of the study as well.[57] RM-493 has also been investigated in a Phase II trial in patients with rare genetic obesities (POMC deficiency, leptin/leptin receptor deficiency, Prader-Willi syndrome, Bardet-Biedl, etc.) clinical trial: NCT03013543. No drugs aimed towards increasing appetite through the melanocortin cascade have made it to the clinic to date.

Within the melanocortin system, many single nucleotide polymorphisms (SNPs) have been identified in the receptors,[51,62-67] agonists,[68,69] and antagonists,[48,70-74] which may be linked to a predisposition for an obese or lean phenotype in humans. Receptor polymorphisms can alter protein conformation or structure thereby decreasing the affinity of the normally

processed ligands.[51,62-66] Mutations within genes that code for the peptide ligands can prevent the peptides from being synthesized or processed properly, alter ligand affinity or activity at the receptor, disrupting the natural signaling cascade and ultimately altering the phenotype of the patient.[68,69,72-76]

This study focused on exploring four single nucleotide polymorphisms that result in missense mutations in the putative active loop of AgRP, containing the Arg-Phe-Phe amino acid motif and the three following residues Asn, Ala, and Phe. This sequence is located on an exposed ß-hairpin loop in the structure of AgRP (Figure 1). [77,78] Truncation studies have demonstrated that the cysteine-rich carboxyl terminus of AgRP is sufficient to modulate receptor activity at the MC3R and MC4R, and possibly the MC5R as discussed above. [19,77,79] In the native sequence the loop is exposed between a disulfide bridge, Figure 1.

The AgRP antagonist, in its native form, is 132 amino acids in length, with five disulfide bonds throughout the carboxyl terminus; however, biologically active AgRP is attributed to residues 87-132.[19,37] Replicating this protein in its entirety or in its active form, to study multiple polymorphisms is costly and labor-intensive, therefore driving the discovery of smaller, more synthetically amenable probes and scaffolds. In 2015, we reported the discovery that the macrocyclic octapeptide AgRP mimetic scaffold, c[Pro-Arg-Phe-Phe-Asn-Ala-Phe-DPro], was reported to have nanomolar potency at the MC4R.[80] This scaffold uses a DPro-Pro head-to-tail cyclization to create a macrocycle ligand postulated to orient the key pharmacophore AGRP based side-chain groups in a similar conformation to that of the native AGRP endogenous antagonist. This macrocycle is smaller by 37 amino acids from AgRP (87-132), and retains nanomolar MC4R antagonist potency. This macrocycle is amenable to substitutions, allowing for the investigation of multiple potentially deleterious mutations within the putative AGRP active loop. The SNPs were accessed from the NIH Variation Viewer in November 2017 (https://www.ncbi.nlm.nih.gov/variation/view/). The mutations are R111H (rs199927717), R111C (rs1012110755), F112Y (rs200972106), and A115V (rs773319622) based upon the full length AGRP amino acid sequence, Figure 2.[81]

These mutations were systematically incorporated and assayed in the macrocyclic octapeptide scaffold. The polymorphisms were also incorporated into the scaffold with the endogenous $Asn^5$ to diaminopropionic acid (Dap) substitution, as this modification was previously reported to be equipotent to AgRP(87-132) at the MC4R.[80] Screening deposited mutations from a publicly available database versus using the genome sequenced from a small subset of an afflicted population, which has previously been the source of polymorphisms,[51,57,58,63,68,69] allows for a broader understanding of the melanocortinergic control of energy homeostasis through the central receptors, and potentially other physiologically relevant functions through the peripheral receptors. In addition, this broad sourcing allows for a greater understanding of the contribution of polymorphisms in monogenic diseases. To fully characterize these SNPs, they would need to be synthesized in the full length of AgRP. It is hypothesized that the octapeptide scaffold can be utilized as a novel tool to screen polymorphisms that may be disruptive to AgRP signaling at the MCRs and provide new chemical probes to investigate MCR physiology *in vivo*. Using the two previously mentioned scaffolds, an eight-compound library was assayed for activity at the

mouse MC1R, MC3R, MC4R, and MC5R and the human MC4R. Compounds were not tested at the MC2R as it has previously only been activated by full-length ACTH.[1,9]

## Results

All peptides were synthesized using a microwave-assisted synthesizer and standard fluorenylmethoxycarbonyl (Fmoc) techniques.[82,83] Peptides were cleaved from the resin and cyclized using BOP and HOBt, with their side chain protecting groups intact as previously described.[38,39,80,84] Peptides were purified to >95% purity using semi-preparative reverse-phase high performance liquid chromatography (RP-HPLC) after removing the protecting groups from the residues. Purity was determined using an analytical RP-HPLC, using two distinct solvent systems, Table 1. Molecular weights were assessed using either MALDI-TOF/TOF or ESI-TOF/MS (University of Minnesota Mass Spectrometry Laboratory), Table 1. The potencies of these compounds in live cell cAMP accumulation assay are reported in Tables 2 and 3. The binding affinities in live cell $^{125}$I-radiolabeled NDP-MSH binding assay are reported in Tables 4 and 5.

### SNP Incorporations, Asn-Substituted Scaffold:

Compound **1 (MDE 6-82-3c)**, which contains the endogenous sequence of AgRP from residues 111-116 (Arg-Phe-Phe-Asn-Ala-Phe), cyclized through a DPro-Pro motif, was previously reported to have antagonist activity at the mMC3R and mMC4R ($pA_2$= 6.3 and 8.2 respectively), inverse agonist activity at the mMC5R, and partially stimulated the mMC1R (25% of NDP-MSH signal at 100 μM).[80] In the present study, this compound was additionally found to possess antagonist activity at the hMC4R ($pA_2$= 8.0) and mMC5R ($pA_2$= 6.4), as well as inverse agonist activity at the hMC4R (Tables 2 and 3).

This scaffold was designed to recreate the active loop of AgRP cyclized through a DPro-Pro motif that had previously been demonstrated to mimic β-hairpin conformations in other macrocyclic peptides.[85] Therefore, this octapeptide scaffold was used to investigate four naturally occurring AgRP SNPs, without synthesizing the full-length peptide [46 residue AgRP(87-132)]. Substitution of the Ala115 with Val (rs773319622) resulted in **ZMK 2-82**. This peptide (**ZMK 2-82**) was able to partially stimulate the mMC1R (23% NDP-MSH signal at 100 μM), and was unable to stimulate the mMC3R, mMC4R, and mMC5R at the concentrations assayed. When assayed as an antagonist at the mMC3R, mMC4R, and mMC5R, **ZMK 2-82** exhibited antagonist activity ($pA_2$= 5.9, 7.2, and 6.1 respectively) and a $pA_2$ of 7.7 at the hMC4R. Replacing the Arg111 to a His (rs199927717) resulted in the peptide **ZMK 2-96**, which partially stimulated the mMC1R (23% at 100 μM) and did not stimulate the mMC3R, mMC4R, or the mMC5R. **ZMK 2-96** did not possess antagonist activity at the mMC3R ($pA_2$ < 5.0) and was a micromolar antagonist at the mMC4R ($pA_2$= 5.3) and hMC4R ($pA_2$= 5.8). Substituting the Phe112 with Tyr (rs200972106) resulted in **ZMK 2-110**, which was unable to stimulate the mMC1R, mMC3R, or mMC4R at the concentrations assayed, but possessed inverse agonist activity at the mMC5R (−35% at 100 μM), a pharmacology previously observed using this scaffold.[38,39] **ZMK 2-110** was a micromolar to sub-micromolar antagonist at the mMC3R, the mMC4R, and the hMC4R ($pA_2$= 5.8, 6.1, and 6.5 respectively). The last peptide synthesized using this scaffold was

**ZMK 3-18**, which contained an Arg111 to Cys (rs1012110755) substitution. This peptide (**ZMK 3-18**) partially stimulated the mMC1R (46% at 100 μM), was unable to stimulate the mMC3R or mMC4R, and possessed inverse agonist activity at the mMC5R (−32% at 100 μM). **ZMK 3-18** did not have antagonist activity at the mMC3R or mMC5R ($pA_2 < 5.0$) but was a micromolar antagonist at the mMC4R ($pA_2$=5.9) and at the hMC4R ($pA_2$=5.8). Binding affinities reflected the functional activity data and ranged from micro to nanomolar affinities, depending on the SNP incorporated, at all receptors assayed. Binding data is summarized in Tables 4 and 5.

### SNP Incorporations, Dap-Substituted Scaffold:

Compound **2 (MDE 6-82-1c)** incorporates the basic amino acid diaminopropionic acid (Dap) at the $Asn^5$ position in the sequence c[-Pro-Arg-Phe-Phe-$Asn^5$-Ala-Phe-DPro] and has been previously reported to be an equipotent antagonist to endogenous AgRP antagonist at the MC4R.[75] Due to the increased potency of **2,** as compared to **1**, it was hypothesized that the potential losses in potency from the SNPs might be better detected in compound **2** as it and AgRP have similar staring potencies than the less potent compound **1**. This macrocycle (**2**) was able to partially stimulate the mMC1R (30%), was unable to stimulate the mMC3R and mMC4R within the assayed concentrations, and possessed inverse agonist activity at the mMC5R and hMC4R. Compound **2** possessed antagonist activity at the mMC3R, mMC4R, mMC5R, and hMC4R with $pA_2$ values of 6.5, 8.7, 7.3, and 8.6 respectively. Replacement of Ala115 (AGRP numbering) with Val resulted in the compound **ZMK 2-85**. This peptide (**ZMK 2-85**) was able to partially stimulate the mMC1R (79% of maximal NDP-MSH signal at 100 μM), the mMC3R (27%), and the mMC4R (37%), and was unable to stimulate the mMC5R. **ZMK 2-85** also possessed antagonist activity at the mMC3R, mMC4R, mMC5R, and hMC4R ($pA_2$= 6.1, 7.5, 6.3, and 7.6 respectively). Substitution of the Arg111 (AGRP numbering) with a His residue produced **ZMK 2-99**, which partially activated the mMC1R (56% at 100 μM) and was unable to stimulate the mMC3R, mMC4R, or the mMC5R. **ZMK 2-99** was a micromolar antagonist at the mMC3R ($pA_2$= 5.4) and mMC4R ($pA_2$= 6.0) and a sub-micromolar antagonist at the hMC4R ($pA_2$= 6.4). Converting the Phe at the 112 position (AGRP numbering) to Tyr, coupled with the Dap substitution resulted in **ZMK 2-112**. This peptide (**ZMK 2-112**) partially stimulated the mMC1R (48% @ 100μM), was unable to stimulate any other receptor assayed, and possessed sub-micromolar antagonist potency at the mMC3R, mMC4R, mMC5R, and hMC4R ($pA_2$= 6.5, 7.3, 6.5, and 7.5 respectively). The last peptide contained an Arg111 (AGRP numbering) to Cys substitution (**ZMK 3-20**). **ZMK 3-20** was the only peptide that acted as a full agonist at the mMC1R, stimulating the receptor to 98% of the NDP-MSH control, with an $EC_{50}$ of 4000 ± 2000 nM. **ZMK 3-20** partially stimulated the mMC3R (29% @ 100μM) and mMC4R (42% @ 100μM) but was unable to stimulate the mMC5R or the hMC4R up to 100 μM concentrations. This peptide did not have any apparent antagonist activity ($pA_2$ <5.0) at the mMC3R, the mMC4R, or the hMC4R at the highest concentrations of antagonists assayed (10μM). All Dap-containing peptides, in general, possessed more potent binding $IC_{50}$ affinities at the receptors assayed compared to their Asn-containing counterparts, which mirrored the cAMP functional data. Binding $IC_{50}$ affinities are reported in Tables 4 and 5.

## Discussion and Conclusions

This work, for the first time, explored human single nucleotide polymorphisms resulting in missense mutations in the purported binding loop of the endogenous AgRP antagonist that were identified from deposited information into the NIH Variation Viewer database. The protein AgRP antagonizes the MC3R and the MC4R in the central nervous system, in addition to functioning as an inverse agonist at the MC4R. These functions prevent the endogenous agonists from binding in the orthosteric receptor domain, which prompts an increase in food intake when administered *in vivo*. AgRP has been reported to have varied pharmacology at the MC5R,[18,19,37] but any potential physiological roles of these data have not been reported. The database SNPs examined herein have not been previously explored to investigate their potential for altering cellular signaling and functional relevance at the MCRs. To examine the potential impact these SNPs have on cAMP signaling at the MCRs, they were incorporated into the octapeptide macrocyclic scaffold c[Pro-Arg-Phe-Phe-Xaa-Ala-Phe-DPro], where Xaa is either Asn or Dap. This scaffold was previously reported to possess nanomolar potency (Asn) or equipotent potency (Dap) to AgRP (87-132) at the mMC4R.[80] This scaffold was chosen for this study to incorporate the four polymorphisms due to its potency and synthetic amenability.

All compounds, except **ZMK 2-110,** were able to partially or fully stimulate the mMC1R, consistent with prior work published utilizing this scaffold.[80,84] All compounds tested resulted in at least a 10-fold decreased antagonist potency at the mMC4R and hMC4R, as compared to the respective control compounds **1** and **2** (Tables 2 and 3), suggesting that SNPs may impact AgRP function. The greatest loss of activity was seen in compounds with substitutions at the Arg position, decreasing potency by at least a 150-fold relative to the parent control compounds. The Arg position has been previously studied in the Arg-Phe-Phe pharmacophore of AgRP.[21] In a structure activity relationship study published on the homologous agouti (ASP) protein, which shares the Arg-Phe-Phe motif, Kiefer *et al.* reported the conclusion that charge contributed to activity at the Arg position, as binding increased as more positive substitutions were used Lys>His>Gln>Ala.[22] The His substitution may maintain a potential positive charge (depending upon local environmental pH), resulting in decreased potency. In the Arg to Cys polymorphisms, the Cys substitution may be disrupting the native disulfide bonds by introducing new disulfide bonds. Ten cysteine residues are found naturally in the carboxyl end of AgRP, which form five bonds, and create a “cysteine knot” structure.[78] Disruption of this structure could potentially alter the conformation of the protein and decrease its ability to bind properly, although the current scaffold does not permit the examination of this hypothesis, since it does not replicate the cysteines of the C-terminal domain. The substitution of Tyr at the Phe112 position exhibited a 110-fold loss in the Asn scaffold and a 25-fold loss in the Dap scaffold, as compared to their respective parent compounds. These findings are consistent with previously reported structure-activity studies using this scaffold, where either a complete loss in antagonist potency or a decrease in potency from the native sequence at the MC4R was described at the Phe112 position when unnatural aromatic amino acids were substituted, with the exception of a Nal(1’) substitution, which maintained the potency of the parent compound.[80] The findings presented herein recapitulate the hypothesis in the field that the Arg-Phe-Phe

sequence is critical for orthosteric binding and activity as previously reported.[20-22] Lastly, the Ala115 containing macrocyclic peptides resulted in 31- and 15-fold decreased antagonist potency. This position appears to be more amenable to substitutions, albeit resulting in a decreased response relative to control compounds. It has been postulated, based upon GPCR homology molecular modeling, that the ligand Ala side chain is juxtaposed a histidine receptor residue of the MC4R (H264, TM6), when AgRP is bound.[86] Previously reported ligand structure-activity studies have postulated that hydrophobic residues and polar residues (specifically Ser) substituted at the Ala115 position maintain at least micromolar antagonist potency (Ser exhibiting nanomolar potency) compared to the parent compound, but acidic residues Glu and Asp ablated antagonist activity at the MC4R.[38] Modeling these SNP containing peptides herein, illustrate the apparent loss of two critical interactions between the Arg wild-type residue within AgRP and Glu100 and Asp126 residues in the MC4R, Figure 3. See Experimental for full description of modeling and ligand docking.

Many of the compounds were inactive when assayed as agonists at the mMC5R, apart from **ZMK 2-110** and **ZMK 3-18**, which demonstrated inverse agonist activity, similar to the parent compounds as previously reported.[80] Based upon the results from the binding studies (Table 4), demonstrating compounds that bound to the MC5R with micromolar binding $IC_{50}$ values, the **1* (MDE 6-82-3c), ZMK 2-82, ZMK 3-18, 2* (MDE 6-82-1c), ZMK 2-85,** and **ZMK 2-112** ligands were tested for MC5R antagonist pharmacology. The **ZMK 2-82**, **ZMK2-85**, and **ZMK2-112** peptides possessed micromolar antagonist potencies at the mMC5R ($pA_2$= 6.1, 6.3, and 6.5, respectively), suggesting that if AgRP has functional activity at the MC5R, these SNP may lead to altered MC5R signaling, Figure 4.

This scaffold may therefore also serve as a lead in the further development of selective and potent MC5R antagonist ligands, which are lacking in the field to date. While the exact physiological role(s) of the ubiquitously expressed MC5R has not been elucidated, it has been linked to exocrine gland function in mice.[14] Additionally, the MC5R has been investigated for its role in muscle glucose uptake[87] and as a treatment for acne (reviewed by Zhang *et al.*).[88] Non-selective MC5R antagonists have previously been reported, including HS024 that inhibits α-MSH-mediated cAMP stimulation at the MC1R, MC3R, MC4R, and MC5R when administered at 100 nM concentrations.[89] Many ligands have been reported to selectively bind to the MC5R,[90,91] although functional antagonist studies were not reported for these compounds. A peptidomimetic macrocycle (PG20N) was reported to be an MC5R antagonist ($pA_2$= 8.3) that did not activate the MC1R and MC4R at concentrations up to 10 μM, and was reported to possess partial agonist activity at the MC3R ($EC_{50}$ = 50 nM; 21% the effect of MTII).[92] PG20N was derived from the synthetic melanocortin agonist MTII and antagonist SHU9119, while the library in the current study was based upon an AgRP template. Utilizing a different starting scaffold may allow the development of more potent and selective MC5R antagonist ligands that can be used to help determine the physiological roles of the MC5R *in vivo*.

The two compounds that were the most active at the mMC1R (Figure 5), **ZMK 2-85** and **ZMK 3-20**, were also able to partially stimulate the mMC3R and mMC4R (27/37% and 29/42% of the maximal NDP-MSH signal respectively).**ZMK 2-85** possessed antagonist pharmacology at the mMC3R, mMC4R, and mMC5R ($pA_2$= 6.1, 7.5, and 6.3 respectively).

Compounds with this activity profile have been previously reported for the melanocortin system.[93] Interestingly, **ZMK 3-20** had no antagonist activity ($pA_2 < 5.0$) at the micromolar concentrations assayed at either the mMC3R or the mMC4R or the hMC4R but was a full micromolar agonist (4 ± 2 μM) at the mMC1R and partially stimulated the mMC4R (42% of NDP-MSH at 100 μM). The Arg to Cys mutation, when incorporated with the basic residue Dap, produced a melanocortin ligand with unique pharmacology as compared to the rest of the library examined herein, which may be an important lead for studying the nuances of each receptor subtype and generating completely selective ligands.

From the findings in this study, it may be speculated that individuals with these polymorphisms express a form of AgRP that results in decreased MC4R potency, which may be ineffective at stimulating hunger, potentially resulting in a lean phenotype; however, the extent of any physiology consequences is not currently known and would need to be further experimentally verified. The scaffold used was an AgRP mimetic, therefore full-length AgRP incorporating the SNPs would need to be synthesized before concluding any physiologically based hypotheses relating the human SNPs and molecular function. There are many redundant mechanisms that nature has established to maintain energy homeostasis and satiety. For example, it has been reported that animals with genetic modifications preventing them from producing AgRP, NPY, or both, still maintain a normal weight, postulated to a result of compensatory pathways involved in the regulation of feeding and satiety homeostasis.[94] Gropp et al. proposed this was likely due to the maintenance of the AgRP/NPY producing neurons in these animals, allowing for alternate compensatory pathways. When the neurons were ablated using diphtheria toxin, animals exhibited the expected phenotype within 24 hours, demonstrating that the AgRP/NPY neurons are mandatory for feeding behavior.[95] However, these experiments represent situations where the signal (AgRP) is absent through neuronal ablation or genetic knockdown. In the case of the SNPs, the signal (AgRP) can transmit to the recipient (MC4R/MC3R), but at a potentially decreased potency. It is unknown what the human phenotype of this circumstance would be. It was apparent from the studies performed herein, that these polymorphisms altered the melanocortin receptor pharmacology from the endogenous sequence when tested in a live cell cAMP based functional assays and binding affinity assays and therefore should be further investigated in patients.

This study reports the first incorporation of deposited human SNPs of the binding loop of AgRP into a functional macrocyclic scaffold to determine the physiological consequences of the polymorphisms, as well as describes the first AgRP-derived mMC5R peptide antagonists. All compounds assayed demonstrated a decrease in antagonist potency at the MC4R compared to parent ligands of the wild-type sequence or the more potent $Asn^5$Dap substitution scaffolds examined. These polymorphisms may represent a functional change when incorporated into the full-length AgRP, potentially altering AgRP signaling in individuals possessing these SNPs. At the MC1R, one compound did not possess agonist activity (**ZMK 2-110**), one ligand was a full agonist (**ZMK 3-20**), and the others partially stimulated it at 100 μM concentrations. Incorporation of the Dap residue at the 114 position (AGRP sequence numbering) did not universally increase MC4R potency (see **ZMK 3-20**) like previously reported.[84] Additionally, both SNPs that change Arg111 (to either His or

Cys) saw the greatest decrease in potency, followed by the Phe112Tyr substitution, recapitulating the hypothesis in the field that the Arg-Phe-Phe(111-113 AGRP numbering) motif is critical for activity. Further phenotypic characterization of individuals possessing these SNPs will be important in determining the relevance of AgRP polymorphisms in the broader context of modulated energy homeostasis.

## Experimental

### Peptide Synthesis:

Peptides were synthesized using standard Fmoc chemistry.[82,83] Coupling reagents 2-(1-H-benzotriazol-1-yl)-1,1,3,3-tetramethyluronium hexafluorophosphate (HBTU), benzotriazol-1-yl-oxy-tris(dimethylamino) phosphonium hexafluorophosphate (BOP), and 1-hydroxybenzotriazole (HOBt), the H-Pro-2-chlorotrityl resin, and Fmoc-protected amino acids were purchased from Peptides International (Louisville, KY). Dichloromethane (DCM), methanol (MeOH), acetonitrile (ACN), dimethylformamide (DMF) and anhydrous ethyl ether were purchased from Fisher (Fairlawn, NJ). Trifluoroacetic acid (TFA), dimethyl sulfoxide (DMSO), piperidine, triisopropylsilane (TIS), and N,N-diisopropylethylamine (DIEA) were purchased from Sigma-Aldrich (St. Louis, MO). All reagents and chemicals were ACS grade or better and were used without further purification.

Peptides were synthesized on a 0.05 mmol scale using H-Pro-2-chlorotrityl resin (0.76 meq/g substitution) using a manual microwave synthesizer (CEM Discover SPS, Matthews, NC). Amino acids were added from carboxyl to amino terminal with two repeated steps consisting of Fmoc removal and amino acid coupling. Fmoc groups were removed with 20% piperidine in DMF for 2 min at room temperature and additionally for 4 min using microwave irradiation at 75°C at 30W. Incoming amino acids (3.1 eq) were installed with HBTU (3 eq) and DIEA (5 eq) with microwave irradiation at either 50°C (His or Cys) or 75°C for 5 min at 30W. Arginine couplings required 5.1 eq of amino acid, 5 eq HBTU, and 7 eq of DIEA and an additional 5 minutes of irradiation time (10 min total). Deprotection and coupling steps were separated by at least four DMF washes and the ninhydrin[96] or chloranil (for Proline )[97] colorimetric assays were used to monitor reaction progress. After synthesis, peptides were cleaved from the resin, maintaining side-chain protecting groups using a 99:1 solution of DCM: TFA for a total of 6 min. The cleavage solution was concentrated under $N_2$ (g) and peptides were precipitated using ice-cold ethyl-ether. Side-chained protected peptides were cyclized head to tail forming an amide bond through the Arg and Pro residues, in DCM using BOP (3 eq) and HOBt (3 eq) at a peptide concentration of 0.33 mg/mL overnight. The DCM was subsequently removed under vacuum. Without further purification, side chain protecting groups were removed using a solution of a 95:2.5:2.5 solution of TFA:$H_2O$:TIS for 2 h. Peptide solution was concentrated under $N_2$ (g) and cyclized peptide was precipitated using ice-cold ethyl-ether. Peptides were purified using RP-HPLC (Shimadzu) configured with a UV detector and a semi-preparative C18 bonded silica column (Vydac 218TP1010, 1 × 25 cm). Peptides were determined to have >95% purity before being assayed. Purity was determined by analytical RP-HPLC (Shimazdu) configured with a photodiode array detector and an analytical C18 silica column (Vydac 218TP104, 0.46 × 25 cm) in two different solvent systems. Molecular mass was determined by MALDI-MS or

ESI-TOF/MS (Applied Biosystems-Sciex 5800 MALDI/TOF/TOF-MS, Bruker BioTOF II ESI-TOF/MS, University of Minnesota Mass Spectrometry Lab).

### cAMP AlphaScreen® Bioassay:

Compounds were dissolved in DMSO, apart from NDP-MSH, which was dissolved in $H_2O$, to a stock concentration of $10^{-2}$ M. The compounds were characterized in HEK293 cells stably expressing the mMC1R, mMC3R, mMC4R, mMC5R, and hMC4R using a cAMP AlphaScreen® assay (Perkin Elmer), following the manufacturers' instructions and as previously described.[80,98] As the MC2R can only be stimulated by ACTH, it was excluded from this study.[1,9] Peptides were assayed first as agonists at the four mouse receptors. Compounds that did not elicit a full agonist response were then assayed as antagonists at the mouse MC3R, MC4R, and MC5R, and the human MC4R. Experiments were performed three independent times performed in duplicate.

To summarize, cells that had reached 75-85% confluency were removed with Versene (Gibco®) and plated at a concentration of 10,000 cells per well in a 384-well plate (Optiplate™), with 10 μL solution of prepared stimulation buffer (1X HBSS, 5 mM HEPES, 0.5 mM IBMX, 0.1% BSA, pH= 7.4) and 0.5 μg of anti-cAMP acceptor beads. 5 μL of peptide containing solutions (concentrations ranging from $10^{-4}$ to $10^{-13}$, ligand potency dependent) was added to the wells to stimulate the cells and cells were incubated for 2 hours in the dark at room temperature. To determine the antagonist activity, cells were incubated with both the potent MCR agonist NDP-MSH (concentrations ranging from $10^{-6}$ to $10^{-12}$) and peptide (concentrations of 10,000 nM, 5,000 nM, 1,000 nM, and 500 nM), using a Schild paradigm.[99]

Following the incubation period, a 10 μL solution containing: 0.5 μg streptavidin coated donor beads, 0.62 μmol biotinylated-cAMP tracers, and lysis buffer (5 mM HEPES, 0.3% Tween-20, 0.1% BSA, pH= 7.4) was added under green-light and incubated for an additional 2 h in the dark and at room temperature. Plates were read on an EnSpire® (Perkin Elmer) using the 384-Alpha plate pre-normalized assay protocol established by the manufacturer.

### $^{125}$I-NDP-MSH Competitive Binding Assay:

Peptide macrocycles were dissolved in DMSO and assayed using stably transfected HEK293 cells at the mMCRs and the hMC4R. The MC2R was excluded from this study. The resulting dose-response binding curves were used to determine the reported $IC_{50}$ values, using a protocol previously described.[100]

Briefly, cells were grown to >90% confluency in a 12-well polystyrene plate (Corning Life Sciences). Culture media was removed, and cells were incubated for 1 hour at 37°C, 5% $CO_2$ with 500 μL solution of 0.1% BSA in Dulbecco's Modified Eagle Medium (DMEM) containing the peptide macrocycles (concentrations ranging from $10^{-4}$ to $10^{-10}$ M) and a constant of 100,000 cpm/well $^{125}$I-NDP-MSH. Post incubation, the media was removed, and the cells were washed and lysed with 500 μL of 0.1 M NaOH and 500 μL of 1% Triton X-100. Cells were incubated with the lysis solution for 10 minutes at room temperature before being transferred to 12mm x 75 mm polystyrene tubes. Radioactivity was quantified using a WIZARD2 automatic gamma counter (PerkinElmer). Specific binding was

determined using nonradioactive NDP-MSH as a positive control, and the specific binding for compounds was normalized to 100% relative to NDP-MSH. Experiments were performed twice with duplicate wells in each experiment.

### Data Analysis:

The $EC_{50}$ and $pA_2$ values obtained from the AlphaScreen™ are representative of the means of duplicates assayed in at least three independent experiments. Compounds that did not possess agonist activity at the mMC3R, mMC4R, or mMC5R were screened as antagonists at these receptors and at the hMC4R. The $EC_{50}$ and $pA_2$ means and standard errors of the means (SEM) were determined using a non-linear least-squares analysis using PRISM software (v4.0, GraphPad Inc.) fit to the collected data. All peptides were assayed as TFA salts and not corrected for peptide weight. Inverse agonism was determined as a percent change from basal compared to the maximal signal of NDP-MSH at 100 μM. The $IC_{50}$ values obtained from the $^{125}$I-NDP-MSH competitive binding assays are representative of the means of duplicates assayed in two independent experiments. The $IC_{50}$ means and standard deviations (SD) were determined using a non-linear least-squares analysis using PRISM software (v4.0, GraphPad Inc).

### Homology models of human MC4R with peptide-based antagonists:

In the absence of crystal structures of melanocortin receptors (MCRs), homology modeling remains a viable alternative for structural analysis of MCR-ligand complexes. In 2005 the first homology model was generated of the inactive conformation of hMC4R in complex with the C-terminal region of hAGRP (PDB ID:2iqv, 2iqr) [86] using distance geometry calculations by DIANA. [101] The model was based on crystal structures of bovine rhodopsin (PDB ID:1gzm) [102], which has only ~15% sequence similarity to hMC4R, the NMR structure of hAGRP (PDB ID: 1hyk, residues 87-132) [103], and experimentally-derived structural restraints.[86] Our subsequent modeling by distance geometry calculations in 2009 [104] was based on the beta-2 adrenergic receptor structure (PDB ID: 2rh1) that has higher (~30%) sequence similarity to hMC4R. Both 1gzm- and 2rh1-based models were rather similar with rmsd 2.2 Å for 240 Cα-atoms, though they demonstrated some helix shift and deviations in intracellular (IL) and extracellular (EL) loop conformations. Structures of ILs generally followed the corresponding templates, EL2 represented just a short interhelical link in extended conformation, EL3 was restricted by two disulfide bridges connecting EL3 to TM6 (C271-C277) and to N-terminus (C40-C279) [86], while EL1 was either unfolded (in 2rh1-based model) or folded into a β-hairpin (in 1gzm-based model).

At present, these models can be substantially updated due to the progress in structural determination of GPCRs and advances in computational methods for homology modeling. Currently, ~50 crystal structures of GPCRs are available and can be used for homology modeling by automated servers, such as SWISS-MODEL [105], Phyre2 [106], RaptorX [107], M4T [108], and IntFOLD. [109] Comparison of results of automated modeling of hMC4R by these servers demonstrated that crystal structures of human lysophospatidic acid receptor 1 (PDB ID: 4z35) [110] and of the human sphingosine 1-phosphate receptor 1 (PDB ID: 3v2y) [111] likely represent the optimal templates, as they are evolutionary closer to MCRs with the highest (~34%) sequence similarity to hMC4R (27-29% sequence identity) and, unlike other

GPCR structures, lack the conserved Pro in the TM5, which is also absent of MCRs. This evolutionarily conserved Pro from TM5 produces a helical aneurism (an α-bulge with 5 residues per turn), which affects the position of the extracellular part of the TM5 and the conformation of the short EL2.

The latest modeling of the hMC4R (UniProtKB ID: P32245, residues 40-317) in the inactive conformation was based on the refinement of the 4z35-based model of hMC4R generated by SWISS-MODEL server. [105] The particular focus was made on the reformation of ELs, as these loops enclose the ligand binding pocket and likely participate in receptor-ligand interactions.[112,113] The procedure included remodeling of EL3 to satisfy disulfide bridge restraints [86] and of the EL1 to exclude helical bulges and interference with N-terminus attached to EL3 via disulfide, as well as the adjustment of side chains to produces their allowed conformations that lack mutual hindrances. The obtained model was refined by energy minimization (100 steps) with CHARMm force field implemented in QUANTA (Accerlys) using a dielectric constant (ε) of 10 and the adopted-basis Newton-Raphson method. After minimization the rmsd between hMC4R model and its structural template (4z35) was 1.6 Å for 208 equivalent Cα-atoms. The 4z35-based model slightly deviated from previous models: rmsd with 1gzm- and 2rh1-based models were 2.2 and 1.8 Å for 240 Cα-atoms, respectively.

### Ligand docking:

The NMR structure of hAGRP (87-132) fragment [103] was used for docking into the new 4z35-based model of hMC4R. The structure of the octapeptide c[Pro-Arg-Phe-Phe-Dap-Ala-Phe-DPro] was produced from the central β-hairpin loop of hAGRP ($^{110}$CRFFNAFC$^{117}$) by modifying C110 to L-Pro, C117 to D-Pro, and N114 to Dap, followed by Pro-DPro cyclization. The model of the octapeptide was refined by energy minimization with QUANTA/CHARMm. The docking of hAGRP (87-132) and compound **2** octapeptide into 4z35-based model of hMC4R was done by superposition of the β-hairpin central loop with its position in previous models followed by manual adjustment of ligand position and side chain orientations to avoid substantial hindrances with receptor residues and to satisfy experimentally-derived ligand-receptor interactions.[86,112-114] The ligand docking pose was subsequently refined using the solid docking module of QUANTA. Finally, the receptor-ligand complexes were shortly minimized using QUANTA/CHARMm (50 steps, using ε of 10 and the adopted-basis Newton-Raphson method).

### Ligand docking mode:

The central loop (110-117) of hAGRP (87-132) and loop-derived octapeptide contain key residues Arg111, Phe112, and Phe113, which are responsible for antagonist properties of these ligands.[80,115] Therefore, positions and interactions of these residues with receptor are critical for the efficient binding of AGRP-derived ligands and locking the receptor in the inactive conformation. In the proposed hMC4R-ligand models, Phe-Phe motif of the ligand display *trans* side chain configuration, which agrees with impaired activity of Tic-substituted analogues of these residues restricted in the *gauche* configuration of the aromatic ring.[80] Observed interactions of the central loop residues are in perfect agreement with experimental data [86,114,116]: Arg111 forms ionic interactions with receptor D126 and E100;

Phe112 form hydrophobic interactions with I129, F261, L265, and F284; Phe113 is in contact with F184; Phe116 forms hydrophobic interactions with F284 and M281. Remarkably, Asn114 from the central loop of AGRP is spatially close to D189 from the EL2, while corresponding Dap of octapeptide forms H-bond and ionic interactions between its amine group and carboxyl group of D189, Figure 6. Besides, patch of positively charged residues (Arg120, Lys121, Arg131 ) from the C-terminal loop are spatially close and may form ionic interactions with EL1 (D111, D113) in compliance with experimental data [113], while residues from the N-terminal loop forms multiple interactions with EL2 and EL3, supporting experimental observations. [112]

## Supplementary Material

Refer to Web version on PubMed Central for supplementary material.

## Acknowledgements:

This work has been supported by NIH Grant R01DK108893. Carrie Haskell-Luevano is a recipient of a 2017 Wallin Neuroscience Discovery Fund Award through the University of Minnesota. Mark D. Ericson is a recipient of an NIH Postdoctoral Fellowship (F32DK108402). Irina D. Pogozheva was funded by the NSF Division of Biological Infrastructure (award 1855425).

## Abbreviations Used:

| | |
|---|---|
| **ACTH** | Adrenocorticotropin Hormone |
| **AgRP** | Agouti-Related Protein |
| **ASP** | Agouti Signaling Protein |
| **GPCR** | G-protein Coupled Receptor |
| **MCR** | Melanocortin Receptor |
| **MC1R** | Melanocortin 1 Receptor |
| **MC3R** | Melanocortin 3 Receptor |
| **MC4R** | Melanocortin 4 Receptor |
| **MC5R** | Melanocortin 5 Receptor |
| **m** | Mouse |
| **h** | Human |
| **Fmoc** | 9-fluorenylmethoxycarbonyl |
| **cAMP** | Cyclic 5’-Adenosine Monophosphate |
| **MSH** | Melanocyte Stimulating Hormone |
| **POMC** | Proopiomelanocortin |

| | |
|---|---|
| **NDP-MSH** | (4-Norleucine-7-D-Phenylalanine)-Ac-Ser-Tyr-Ser-Nle-Glu-His-DPhe-Arg-Trp-Gly-Lys-Pro-Val-$NH_2$ |
| **Dap** | Diaminopropionic acid |
| **RP-HPLC** | Reverse Phase- High Performance Liquid Chromatography |
| **DMEM** | Dulbecco's Modified Eagle Medium; SEM, Standard Error of the Mean; SD, Standard Deviation |

## References


1. Mountjoy KG; Robbins LS; Mortrud MT; Cone RD The cloning of a family of genes that encode the melanocortin receptors. Science 1992, 257, 1248–1251. [PubMed: 1325670]
2. Chhajlani V; Wikberg JE Molecular cloning and expression of the human melanocyte stimulating hormone receptor cDNA. FEBS Lett 1992, 309, 417–420. [PubMed: 1516719]
3. Gantz I; Konda Y; Tashiro T; Shimoto Y; Miwa H; Munzert G; Watson SJ; DelValle J; Yamada T Molecular cloning of a novel melanocortin receptor. J Biol Chem 1993, 268, 8246–8250. [PubMed: 8463333]
4. Gantz I; Miwa H; Konda Y; Shimoto Y; Tashiro T; Watson SJ; DelValle J; Yamada T Molecular cloning, expression, and gene localization of a fourth melanocortin receptor. J Biol Chem 1993, 268, 15174–15179. [PubMed: 8392067]
5. Roselli-Rehfuss L; Mountjoy KG; Robbins LS; Mortrud MT; Low MJ; Tatro JB; Entwistle ML; Simerly RB; Cone RD Identification of a receptor for gamma melanotropin and other proopiomelanocortin peptides in the hypothalamus and limbic system. Proc Natl Acad Sci U S A 1993, 90, 8856–8860. [PubMed: 8415620]
6. Gantz I; Shimoto Y; Konda Y; Miwa H; Dickinson CJ; Yamada T Molecular cloning, expression, and characterization of a fifth melanocortin receptor. Biochem Biophys Res Commun 1994, 200, 1214–1220. [PubMed: 8185570]
7. Griffon N; Mignon V; Facchinetti P; Diaz J; Schwartz JC; Sokoloff P Molecular cloning and characterization of the rat fifth melanocortin receptor. Biochem Biophys Res Commun 1994, 200, 1007–1014. [PubMed: 8179577]
8. Chhajlani V; Muceniece R; Wikberg JE Molecular cloning of a novel human melanocortin receptor. Biochem Biophys Res Commun 1993, 195, 866–873. [PubMed: 8396929]
9. Haynes RC Jr.; Berthet L Studies on the mechanism of action of the adrenocorticotropic hormone. J Biol Chem 1957, 225, 115–124. [PubMed: 13416222]
10. Chen AS; Marsh DJ; Trumbauer ME; Frazier EG; Guan XM; Yu H; Rosenblum CI; Vongs A; Feng Y; Cao L; Metzger JM; Strack AM; Camacho RE; Mellin TN; Nunes CN; Min W; Fisher J; Gopal-Truter S; MacIntyre DE; Chen HY; Van der Ploeg LH Inactivation of the mouse melanocortin-3 receptor results in increased fat mass and reduced lean body mass. Nat Genet 2000, 26, 97–102. [PubMed: 10973258]
11. Butler AA; Kesterson RA; Khong K; Cullen MJ; Pelleymounter MA; Dekoning J; Baetscher M; Cone RD A unique metabolic syndrome causes obesity in the melanocortin-3 receptor-deficient mouse. Endocrinology 2000, 141, 3518–3521. [PubMed: 10965927]
12. Irani BG; Xiang Z; Yarandi HN; Holder JR; Moore MC; Bauzo RM; Proneth B; Shaw AM; Millard WJ; Chambers JB; Benoit SC; Clegg DJ; Haskell-Luevano C Implication of the melanocortin-3 receptor in the regulation of food intake. Eur J Pharmacol 2011, 660, 80–87. [PubMed: 21199647]
13. Huszar D; Lynch CA; Fairchild-Huntress V; Dunmore JH; Fang Q; Berkemeier LR; Gu W; Kesterson RA; Boston BA; Cone RD; Smith FJ; Campfield LA; Burn P; Lee F Targeted disruption of the melanocortin-4 receptor results in obesity in mice. Cell 1997, 88, 131–141. [PubMed: 9019399]

14. Chen W; Kelly MA; Opitz-Araya X; Thomas RE; Low MJ; Cone RD Exocrine gland dysfunction in MC5-R-deficient mice: evidence for coordinated regulation of exocrine gland function by melanocortin peptides. Cell 1997, 91, 789–798. [PubMed: 9413988]
15. Nakanishi S; Inoue A; Kita T; Nakamura M; Chang AC; Cohen SN; Numa S Nucleotide sequence of cloned cDNA for bovine corticotropin-beta-lipotropin precursor. Nature 1979, 278, 423–427. [PubMed: 221818]
16. Bultman SJ; Michaud EJ; Woychik RP Molecular characterization of the mouse agouti locus. Cell 1992, 71, 1195–1204. [PubMed: 1473152]
17. Miller MW; Duhl DM; Vrieling H; Cordes SP; Ollmann MM; Winkes BM; Barsh GS Cloning of the mouse agouti gene predicts a secreted protein ubiquitously expressed in mice carrying the lethal yellow mutation. Genes Dev 1993, 7, 454–467. [PubMed: 8449404]
18. Fong TM; Mao C; MacNeil T; Kalyani R; Smith T; Weinberg D; Tota MR; Van der Ploeg LH ART (protein product of agouti-related transcript) as an antagonist of MC-3 and MC-4 receptors. Biochem Biophys Res Commun 1997, 237, 629–631. [PubMed: 9299416]
19. Ollmann MM; Wilson BD; Yang YK; Kerns JA; Chen Y; Gantz I; Barsh GS Antagonism of central melanocortin receptors in vitro and in vivo by agouti-related protein. Science 1997, 278, 135–138. [PubMed: 9311920]
20. Dinulescu DM; Cone RD Agouti and agouti-related protein: analogies and contrasts. J Biol Chem 2000, 275, 6695–6698. [PubMed: 10702221]
21. Tota MR; Smith TS; Mao C; MacNeil T; Mosley RT; Van der Ploeg LH; Fong TM Molecular interaction of Agouti protein and Agouti-related protein with human melanocortin receptors. Biochemistry 1999, 38, 897–904. [PubMed: 9893984]
22. Kiefer LL; Veal JM; Mountjoy KG; Wilkison WO Melanocortin receptor binding determinants in the agouti protein. Biochemistry 1998, 37, 991–997. [PubMed: 9454589]
23. Mountjoy KG; Mortrud MT; Low MJ; Simerly RB; Cone RD Localization of the melanocortin-4 receptor (MC4-R) in neuroendocrine and autonomic control circuits in the brain. Mol Endocrinol 1994, 8, 1298–1308. [PubMed: 7854347]
24. Fan W; Boston BA; Kesterson RA; Hruby VJ; Cone RD Role of melanocortinergic neurons in feeding and the agouti obesity syndrome. Nature 1997, 385, 165–168. [PubMed: 8990120]
25. Giraudo SQ; Billington CJ; Levine AS Feeding effects of hypothalamic injection of melanocortin 4 receptor ligands. Brain Res 1998, 809, 302–306. [PubMed: 9853124]
26. Morton GJ; Schwartz MW The NPY/AgRP neuron and energy homeostasis. Int J Obes Relat Metab Disord 2001, 25 Suppl 5, S56–62.
27. Nijenhuis WA; Oosterom J; Adan RA AgRP(83–132) acts as an inverse agonist on the human-melanocortin-4 receptor. Mol Endocrinol 2001, 15, 164–171. [PubMed: 11145747]
28. Haskell-Luevano C; Monck EK Agouti-related protein functions as an inverse agonist at a constitutively active brain melanocortin-4 receptor. Regul Pept 2001, 99, 1–7. [PubMed: 11257308]
29. Sawyer TK; Sanfilippo PJ; Hruby VJ; Engel MH; Heward CB; Burnett JB; Hadley ME 4-Norleucine, 7-D-phenylalanine-alpha-melanocyte-stimulating hormone: a highly potent alpha-melanotropin with ultralong biological activity. Proc Natl Acad Sci U S A 1980, 77, 5754–5758. [PubMed: 6777774]
30. Al-Obeidi F; Castrucci AM; Hadley ME; Hruby VJ Potent and prolonged acting cyclic lactam analogues of alpha-melanotropin: design based on molecular dynamics. J Med Chem 1989, 32, 2555–2561. [PubMed: 2555512]
31. Pierroz DD; Ziotopoulou M; Ungsunan L; Moschos S; Flier JS; Mantzoros CS Effects of acute and chronic administration of the melanocortin agonist MTII in mice with diet-induced obesity. Diabetes 2002, 51, 1337–1345. [PubMed: 11978628]
32. Adank DN; Lunzer MM; Lensing CJ; Wilber SL; Gancarz AM; Haskell-Luevano C Comparative in vivo investigation of intrathecal and intracerebroventricular administration with melanocortin ligands MTII and AGRP into mice. ACS Chem Neurosci 2018, 9, 320–327. [PubMed: 28968061]
33. Chen AS; Metzger JM; Trumbauer ME; Guan XM; Yu H; Frazier EG; Marsh DJ; Forrest MJ; Gopal-Truter S; Fisher J; Camacho RE; Strack AM; Mellin TN; MacIntyre DE; Chen HY; Van der

Ploeg LH Role of the melanocortin-4 receptor in metabolic rate and food intake in mice. Transgenic Res 2000, 9, 145–154. [PubMed: 10951699]

34. Kim MS; Rossi M; Abusnana S; Sunter D; Morgan DG; Small CJ; Edwards CM; Heath MM; Stanley SA; Seal LJ; Bhatti JR; Smith DM; Ghatei MA; Bloom SR Hypothalamic localization of the feeding effect of agouti-related peptide and alpha-melanocyte-stimulating hormone. Diabetes 2000, 49, 177–182. [PubMed: 10868932]
35. Wirth MM; Giraudo SQ Agouti-related protein in the hypothalamic paraventricular nucleus: effect on feeding. Peptides 2000, 21, 1369–1375. [PubMed: 11072124]
36. Hagan MM; Rushing PA; Pritchard LM; Schwartz MW; Strack AM; Van Der Ploeg LH; Woods SC; Seeley RJ Long-term orexigenic effects of AgRP-(83-−-132) involve mechanisms other than melanocortin receptor blockade. Am J Physiol Regul Integr Comp Physiol 2000, 279, R47–52. [PubMed: 10896863]
37. Yang YK; Thompson DA; Dickinson CJ; Wilken J; Barsh GS; Kent SB; Gantz I Characterization of Agouti-related protein binding to melanocortin receptors. Mol Endocrinol 1999, 13, 148–155. [PubMed: 9892020]
38. Ericson MD; Freeman KT; Schnell SM; Fleming KA; Haskell-Luevano C Structure-activity relationship studies on a macrocyclic Agouti-Related Protein (AGRP) scaffold reveal Agouti Signaling Protein (ASP) residue substitutions maintain melanocortin-4 receptor antagonist potency and result in inverse agonist pharmacology at the melanocortin-5 receptor. J Med Chem 2017, 60, 8103–8114. [PubMed: 28813605]
39. Fleming KA; Ericson MD; Freeman KT; Adank DN; Lunzer MM; Wilber SL; Haskell-Luevano C Structure-activity relationship studies of a macrocyclic AGRP-mimetic scaffold c[Pro-Arg-Phe-Phe-Asn-Ala-Phe-DPro] yield potent and selective melanocortin-4 receptor antagonists and melanocortin-5 receptor inverse agonists that increase food intake in mice. ACS Chem Neurosci 2018, 9, 1141–1151. [PubMed: 29363944]
40. Al-Obeidi F; Hadley ME; Pettitt BM; Hruby VJ Design of a new class of superpotent cyclic alpha-melanotropins based on quenched dynamic simulations. J Am Chem Soc 1989, 111, 3413–3416.
41. Lan EL; Ugwu SO; Blanchard J; Fang X; Hruby VJ; Sharma S Preformulation studies with melanotan-II: a potential skin cancer chemopreventive peptide. J Pharm Sci 1994, 83, 1081–1084. [PubMed: 7983590]
42. Levine N; Sheftel SN; Eytan T; Dorr RT; Hadley ME; Weinrach JC; Ertl GA; Toth K; McGee DL; Hruby VJ Induction of skin tanning by subcutaneous administration of a potent synthetic melanotropin. JAMA 1991, 266, 2730–2736. [PubMed: 1658407]
43. Levine N; Lemus-Wilson A; Wood SH; Abdel Malek ZA; Al-Obeidi F; Hruby VJ; Hadley ME Stimulation of follicular melanogenesis in the mouse by topical and injected melanotropins. J Invest Dermatol 1987, 89, 269–273. [PubMed: 3624899]
44. Hadley ME; Hruby VJ; Jiang J; Sharma SD; Fink JL; Haskell-Luevano C; Bentley DL; al-Obeidi F; Sawyer TK Melanocortin receptors: identification and characterization by melanotropic peptide agonists and antagonists. Pigment Cell Res 1996, 9, 213–234. [PubMed: 9014208]
45. Lubrano-Berthelier C; Cavazos M; Le Stunff C; Haas K; Shapiro A; Zhang S; Bougneres P; Vaisse C The human MC4R promoter: characterization and role in obesity. Diabetes 2003, 52, 2996–3000. [PubMed: 14633862]
46. Butler AA; Cone RD Knockout models resulting in the development of obesity. Trends Genet 2001, 17, S50–54. [PubMed: 11585677]
47. Wisse BE; Frayo RS; Schwartz MW; Cummings DE Reversal of cancer anorexia by blockade of central melanocortin receptors in rats. Endocrinology 2001, 142, 3292–3301. [PubMed: 11459770]
48. Vink T; Hinney A; van Elburg AA; van Goozen SH; Sandkuijl LA; Sinke RJ; Herpertz-Dahlmann BM; Hebebrand J; Remschmidt H; van Engeland H; Adan RA Association between an agouti-related protein gene polymorphism and anorexia nervosa. Mol Psychiatry 2001, 6, 325–328. [PubMed: 11326303]
49. Marks DL; Ling N; Cone RD Role of the central melanocortin system in cachexia. Cancer Res 2001, 61, 1432–1438. [PubMed: 11245447]
50. Finkelstein EA; Khavjou OA; Thompson H; Trogdon JG; Pan L; Sherry B; Dietz W Obesity and severe obesity forecasts through 2030. Am J Prev Med 2012, 42, 563–570. [PubMed: 22608371]

51. Vaisse C; Clement K; Durand E; Hercberg S; Guy-Grand B; Froguel P Melanocortin-4 receptor mutations are a frequent and heterogeneous cause of morbid obesity. J Clin Invest 2000, 106, 253–262. [PubMed: 10903341]
52. Farooqi IS; Keogh JM; Yeo GS; Lank EJ; Cheetham T; O'Rahilly S Clinical spectrum of obesity and mutations in the melanocortin 4 receptor gene. N Engl J Med 2003, 348, 1085–1095. [PubMed: 12646665]
53. Yeo GS; Lank EJ; Farooqi IS; Keogh J; Challis BG; O'Rahilly S Mutations in the human melanocortin-4 receptor gene associated with severe familial obesity disrupts receptor function through multiple molecular mechanisms. Hum Mol Genet 2003, 12, 561–574. [PubMed: 12588803]
54. Weyermann P; Dallmann R; Magyar J; Anklin C; Hufschmid M; Dubach-Powell J; Courdier-Fruh I; Hennebohle M; Nordhoff S; Mondadori C Orally available selective melanocortin-4 receptor antagonists stimulate food intake and reduce cancer-induced cachexia in mice. PLoS One 2009, 4, e4774. [PubMed: 19295909]
55. Ge Y; Ohta T; Driscoll DJ; Nicholls RD; Kalra SP Anorexigenic melanocortin signaling in the hypothalamus is augmented in association with failure-to-thrive in a transgenic mouse model for Prader-Willi syndrome. Brain Res 2002, 957, 42–45. [PubMed: 12443978]
56. Greenfield JR; Miller JW; Keogh JM; Henning E; Satterwhite JH; Cameron GS; Astruc B; Mayer JP; Brage S; See TC; Lomas DJ; O'Rahilly S; Farooqi IS Modulation of blood pressure by central melanocortinergic pathways. N Engl J Med 2009, 360, 44–52. [PubMed: 19092146]
57. Kuhnen P; Clement K; Wiegand S; Blankenstein O; Gottesdiener K; Martini LL; Mai K; Blume-Peytavi U; Gruters A; Krude H Proopiomelanocortin deficiency treated with a melanocortin-4 receptor agonist. N Engl J Med 2016, 375, 240–246. [PubMed: 27468060]
58. Clement K; Biebermann H; Farooqi IS; Van der Ploeg L; Wolters B; Poitou C; Puder L; Fiedorek F; Gottesdiener K; Kleinau G; Heyder N; Scheerer P; Blume-Peytavi U; Jahnke I; Sharma S; Mokrosinski J; Wiegand S; Muller A; Weiss K; Mai K; Spranger J; Gruters A; Blankenstein O; Krude H; Kuhnen P MC4R agonism promotes durable weight loss in patients with leptin receptor deficiency. Nat Med 2018, 24, 551–555. [PubMed: 29736023]
59. Dorr RT; Lines R; Levine N; Brooks C; Xiang L; Hruby VJ; Hadley ME Evaluation of melanotan-II, a superpotent cyclic melanotropic peptide in a pilot phase-I clinical study. Life Sci 1996, 58, 1777–1784. [PubMed: 8637402]
60. Ericson MD; Lensing CJ; Fleming KA; Schlasner KN; Doering SR; Haskell-Luevano C Bench-top to clinical therapies: A review of melanocortin ligands from 1954 to 2016. Biochim Biophys Acta Mol Basis Dis 2017, 1863, 2414–2435. [PubMed: 28363699]
61. Chen KY; Muniyappa R; Abel BS; Mullins KP; Staker P; Brychta RJ; Zhao X; Ring M; Psota TL; Cone RD; Panaro BL; Gottesdiener KM; Van der Ploeg LH; Reitman ML; Skarulis MC RM-493, a melanocortin-4 receptor (MC4R) agonist, increases resting energy expenditure in obese individuals. J Clin Endocrinol Metab 2015, 100, 1639–1645. [PubMed: 25675384]
62. Yeo GS; Farooqi IS; Aminian S; Halsall DJ; Stanhope RG; O'Rahilly S A frameshift mutation in MC4R associated with dominantly inherited human obesity. Nat Genet 1998, 20, 111–112. [PubMed: 9771698]
63. Vaisse C; Clement K; Guy-Grand B; Froguel P A frameshift mutation in human MC4R is associated with a dominant form of obesity. Nat Genet 1998, 20, 113–114. [PubMed: 9771699]
64. Feng N; Young SF; Aguilera G; Puricelli E; Adler-Wailes DC; Sebring NG; Yanovski JA Co-occurrence of two partially inactivating polymorphisms of MC3R is associated with pediatric-onset obesity. Diabetes 2005, 54, 2663–2667. [PubMed: 16123355]
65. Mencarelli M; Walker GE; Maestrini S; Alberti L; Verti B; Brunani A; Petroni ML; Tagliaferri M; Liuzzi A; Di Blasio AM Sporadic mutations in melanocortin receptor 3 in morbid obese individuals. Eur J Hum Genet 2008, 16, 581–586. [PubMed: 18231126]
66. Wong J; Love DR; Kyle C; Daniels A; White M; Stewart AW; Schnell AH; Elston RC; Holdaway IM; Mountjoy KG Melanocortin-3 receptor gene variants in a Maori kindred with obesity and early onset type 2 diabetes. Diabetes Res Clin Pract 2002, 58, 61–71. [PubMed: 12161058]
67. Santos JL; De la Cruz R; Holst C; Grau K; Naranjo C; Maiz A; Astrup A; Saris WH; MacDonald I; Oppert JM; Hansen T; Pedersen O; Sorensen TI; Martinez JA; Consortium N Allelic variants of

melanocortin 3 receptor gene (MC3R) and weight loss in obesity: a randomised trial of hypo-energetic high- versus low-fat diets. PLoS One 2011, 6, e19934. [PubMed: 21695122]

68. Krude H; Biebermann H; Luck W; Horn R; Brabant G; Gruters A Severe early-onset obesity, adrenal insufficiency and red hair pigmentation caused by POMC mutations in humans. Nat Genet 1998, 19, 155–157. [PubMed: 9620771]
69. Challis BG; Pritchard LE; Creemers JW; Delplanque J; Keogh JM; Luan J; Wareham NJ; Yeo GS; Bhattacharyya S; Froguel P; White A; Farooqi IS; O'Rahilly S A missense mutation disrupting a dibasic prohormone processing site in pro-opiomelanocortin (POMC) increases susceptibility to early-onset obesity through a novel molecular mechanism. Hum Mol Genet 2002, 11, 1997–2004. [PubMed: 12165561]
70. Argyropoulos G; Rankinen T; Neufeld DR; Rice T; Province MA; Leon AS; Skinner JS; Wilmore JH; Rao DC; Bouchard C A polymorphism in the human agouti-related protein is associated with late-onset obesity. J Clin Endocrinol Metab 2002, 87, 4198–4202. [PubMed: 12213871]
71. Marks DL; Boucher N; Lanouette CM; Perusse L; Brookhart G; Comuzzie AG; Chagnon YC; Cone RD Ala67Thr polymorphism in the Agouti-related peptide gene is associated with inherited leanness in humans. Am J Med Genet A 2004, 126A, 267–271. [PubMed: 15054840]
72. Kalnina I; Kapa I; Pirags V; Ignatovica V; Schioth HB; Klovins J Association between a rare SNP in the second intron of human Agouti related protein gene and increased BMI. BMC Med Genet 2009, 10, 63. [PubMed: 19602223]
73. de Rijke CE; Jackson PJ; Garner KM; van Rozen RJ; Douglas NR; Kas MJ; Millhauser GL; Adan RA Functional analysis of the Ala67Thr polymorphism in agouti related protein associated with anorexia nervosa and leanness. Biochem Pharmacol 2005, 70, 308–316. [PubMed: 15927146]
74. Bonilla C; Panguluri RK; Taliaferro-Smith L; Argyropoulos G; Chen G; Adeyemo AA; Amoah A; Owusu S; Acheampong J; Agyenim-Boateng K; Eghan BA; Oli J; Okafor G; Abbiyesuku F; Johnson T; Rufus T; Fasanmade O; Chen Y; Collins FS; Dunston GM; Rotimi C; Kittles RA Agouti-related protein promoter variant associated with leanness and decreased risk for diabetes in West Africans. Int J Obes (Lond) 2006, 30, 715–721. [PubMed: 16130030]
75. Li P; Tiwari HK; Lin WY; Allison DB; Chung WK; Leibel RL; Yi N; Liu N Genetic association analysis of 30 genes related to obesity in a European American population. Int J Obes (Lond) 2014, 38, 724–729. [PubMed: 23900445]
76. Ilnytska O; Argyropoulos G The role of the Agouti-related protein in energy balance regulation. Cell Mol Life Sci 2008, 65, 2721–2731. [PubMed: 18470724]
77. Millhauser GL; McNulty JC; Jackson PJ; Thompson DA; Barsh GS; Gantz I Loops and links: structural insights into the remarkable function of the agouti-related protein. Ann N Y Acad Sci 2003, 994, 27–35. [PubMed: 12851295]
78. Bolin KA; Anderson DJ; Trulson JA; Thompson DA; Wilken J; Kent SB; Gantz I; Millhauser GL NMR structure of a minimized human agouti related protein prepared by total chemical synthesis. FEBS Lett 1999, 451, 125–131. [PubMed: 10371151]
79. Quillan JM; Sadee W; Wei ET; Jimenez C; Ji L; Chang JK A synthetic human Agouti-related protein-(83–132)-NH2 fragment is a potent inhibitor of melanocortin receptor function. FEBS Lett 1998, 428, 59–62. [PubMed: 9645475]
80. Ericson MD; Wilczynski A; Sorensen NB; Xiang Z; Haskell-Luevano C Discovery of a beta-Hairpin Octapeptide, c[Pro-Arg-Phe-Phe-Dap-Ala-Phe-DPro], Mimetic of Agouti-Related Protein(87–132) [AGRP(87–132)] with Equipotent Mouse Melanocortin-4 Receptor (mMC4R) Antagonist Pharmacology. J Med Chem 2015, 58, 4638–4647. [PubMed: 25898270]
81. Ericson MD; Haskell-Luevano C A review of single-nucleotide polymorphisms in orexigenic neuropeptides targeting G protein-coupled receptors. ACS Chem Neurosci 2018, 9, 1235–1246. [PubMed: 29714060]
82. Carpino LA; Han GY 9-Fluorenylmethoxycarbonyl function, a new base-sensitive amino-protecting group. J Am Chem Soc 1970, 92, 5748-&.
83. Carpino LA; Han GY 9-Fluorenylmethoxycarbonyl amino-protecting group. J Org Chem 1972, 37, 3404-&.
84. Ericson MD; Koerperich ZM; Freeman KT; Fleming KA; Haskell-Luevano C Arg-Phe-Phe D-amino acid stereochemistry scan in the macrocyclic Agouti-related protein antagonist scaffold

c[Pro-Arg-Phe-Phe-Xxx-Ala-Phe-DPro] results in unanticipated melanocortin-1 receptor agonist profiles. ACS Chem Neurosci 2018, 9, 3015–3023. [PubMed: 29924583]

85. Jiang LJ; Moehle K; Dhanapal B; Obrecht D; Robinson JA Combinatorial biomimetic chemistry: parallel synthesis of a small library of beta-hairpin mimetics based on loop III from human platelet-derived growth factor B. Helvetica Chimica Acta 2000, 83, 3097–3112.
86. Chai BX; Pogozheva ID; Lai YM; Li JY; Neubig RR; Mosberg HI; Gantz I Receptor-antagonist interactions in the complexes of agouti and agouti-related protein with human melanocortin 1 and 4 receptors. Biochemistry 2005, 44, 3418–3431. [PubMed: 15736952]
87. Enriori PJ; Chen W; Garcia-Rudaz MC; Grayson BE; Evans AE; Comstock SM; Gebhardt U; Muller HL; Reinehr T; Henry BA; Brown RD; Bruce CR; Simonds SE; Litwak SA; McGee SL; Luquet S; Martinez S; Jastroch M; Tschop MH; Watt MJ; Clarke IJ; Roth CL; Grove KL; Cowley MA alpha-Melanocyte stimulating hormone promotes muscle glucose uptake via melanocortin 5 receptors. Mol Metab 2016, 5, 807–822. [PubMed: 27688995]
88. Zhang L; Li WH; Anthonavage M; Pappas A; Rossetti D; Cavender D; Seiberg M; Eisinger M Melanocortin-5 receptor and sebogenesis. Eur J Pharmacol 2011, 660, 202–206. [PubMed: 21215742]
89. Kask A; Mutulis F; Muceniece R; Pahkla R; Mutule I; Wikberg JE; Rago L; Schioth HB Discovery of a novel superpotent and selective melanocortin-4 receptor antagonist (HS024): evaluation in vitro and in vivo. Endocrinology 1998, 139, 5006–5014. [PubMed: 9832440]
90. Balse-Srinivasan P; Grieco P; Cai MY; Trivedi D; Hruby VJ Structure-activity relationships of novel cyclic alpha-MSH/beta-MSH hybrid analogues that lead to potent and selective ligands for the human MC3R and human MC5R. J Med Chem 2003, 46, 3728–3733. [PubMed: 12904077]
91. Cain JP; Mayorov AV; Cai M; Wang H; Tan B; Chandler K; Lee Y; Petrov RR; Trivedi D; Hruby VJ Design, synthesis, and biological evaluation of a new class of small molecule peptide mimetics targeting the melanocortin receptors. Bioorg Med Chem Lett 2006, 16, 5462–5467. [PubMed: 16931008]
92. Grieco P; Cai M; Liu L; Mayorov A; Chandler K; Trivedi D; Lin G; Campiglia P; Novellino E; Hruby VJ Design and microwave-assisted synthesis of novel macrocyclic peptides active at melanocortin receptors: discovery of potent and selective hMC5R receptor antagonists. J Med Chem 2008, 51, 2701–2707. [PubMed: 18412316]
93. Hruby VJ; Lu D; Sharma SD; Castrucci AL; Kesterson RA; al-Obeidi FA; Hadley ME; Cone RD Cyclic lactam alpha-melanotropin analogues of Ac-Nle4-cyclo[Asp5, D-Phe7,Lys10] alpha-melanocyte-stimulating hormone-(4–10)-NH2 with bulky aromatic amino acids at position 7 show high antagonist potency and selectivity at specific melanocortin receptors. J Med Chem 1995, 38, 3454–3461. [PubMed: 7658432]
94. Qian S; Chen H; Weingarth D; Trumbauer ME; Novi DE; Guan X; Yu H; Shen Z; Feng Y; Frazier E; Chen A; Camacho RE; Shearman LP; Gopal-Truter S; MacNeil DJ; Van der Ploeg LH; Marsh DJ Neither agouti-related protein nor neuropeptide Y is critically required for the regulation of energy homeostasis in mice. Mol Cell Biol 2002, 22, 5027–5035. [PubMed: 12077332]
95. Gropp E; Shanabrough M; Borok E; Xu AW; Janoschek R; Buch T; Plum L; Balthasar N; Hampel B; Waisman A; Barsh GS; Horvath TL; Bruning JC Agouti-related peptide-expressing neurons are mandatory for feeding. Nat Neurosci 2005, 8, 1289–1291. [PubMed: 16158063]
96. Kaiser E; Colescott RL; Bossinger CD; Cook PI Color test for detection of free terminal amino groups in the solid-phase synthesis of peptides. Anal Biochem 1970, 34, 595–598. [PubMed: 5443684]
97. Christensen T Qualitative test for monitoring coupling completeness in solid-phase peptide-synthesis using chloranil. Acta Chem Scand 1979, 33, 763–766.
98. Lensing CJ; Freeman KT; Schnell SM; Adank DN; Speth RC; Haskell-Luevano C An in vitro and in vivo investigation of bivalent ligands that display preferential binding and functional activity for different melanocortin receptor homodimers. J Med Chem 2016, 59, 3112–3128. [PubMed: 26959173]
99. Schild HO pA, a new scale for the measurement of drug antagonism. Br J Pharmacol Chemother 1947, 2, 189–206. [PubMed: 20258355]

100. Doering SR; Freeman KT; Schnell SM; Haslach EM; Dirain M; Debevec G; Geer P; Santos RG; Giulianotti MA; Pinilla C; Appel JR; Speth RC; Houghten RA; Haskell-Luevano C Discovery of mixed pharmacology melanocortin-3 agonists and melanocortin-4 receptor tetrapeptide antagonist compounds (TACOs) based on the sequence Ac-Xaa(1)-Arg-(pI)DPhe-Xaa(4)-NH2. J Med Chem 2017, 60, 4342–4357. [PubMed: 28453292]

101. Guntert P; Braun W; Wuthrich K Efficient computation of three-dimensional protein structures in solution from nuclear magnetic resonance data using the program DIANA and the supporting programs CALIBA, HABAS and GLOMSA. J Mol Biol 1991, 217, 517–530. [PubMed: 1847217]

102. Li J; Edwards PC; Burghammer M; Villa C; Schertler GF Structure of bovine rhodopsin in a trigonal crystal form. J Mol Biol 2004, 343, 1409–1438. [PubMed: 15491621]

103. McNulty JC; Thompson DA; Bolin KA; Wilken J; Barsh GS; Millhauser GL High-resolution NMR structure of the chemically-synthesized melanocortin receptor binding domain AGRP(87–132) of the agouti-related protein. Biochemistry 2001, 40, 15520–15527. [PubMed: 11747427]

104. Tan K; Pogozheva ID; Yeo GS; Hadaschik D; Keogh JM; Haskell-Leuvano C; O'Rahilly S; Mosberg HI; Farooqi IS Functional characterization and structural modeling of obesity associated mutations in the melanocortin 4 receptor. Endocrinology 2009, 150, 114–125. [PubMed: 18801902]

105. Biasini M; Bienert S; Waterhouse A; Arnold K; Studer G; Schmidt T; Kiefer F; Cassarino TG; Bertoni M; Bordoli L; Schwede T SWISS-MODEL: modelling protein tertiary and quaternary structure using evolutionary information. Nucleic Acids Res 2014, 42, W252–258. [PubMed: 24782522]

106. Kelley LA; Mezulis S; Yates CM; Wass MN; Sternberg MJ The Phyre2 web portal for protein modeling, prediction and analysis. Nat Protoc 2015, 10, 845–858. [PubMed: 25950237]

107. Kallberg M; Wang H; Wang S; Peng J; Wang Z; Lu H; Xu J Template-based protein structure modeling using the RaptorX web server. Nat Protoc 2012, 7, 1511–1522. [PubMed: 22814390]

108. Fernandez-Fuentes N; Madrid-Aliste CJ; Rai BK; Fajardo JE; Fiser A M4T: a comparative protein structure modeling server. Nucleic Acids Res 2007, 35, W363–368. [PubMed: 17517764]

109. Roche DB; Buenavista MT; Tetchner SJ; McGuffin LJ The IntFOLD server: an integrated web resource for protein fold recognition, 3D model quality assessment, intrinsic disorder prediction, domain prediction and ligand binding site prediction. Nucleic Acids Res 2011, 39, W171–176. [PubMed: 21459847]

110. Chrencik JE; Roth CB; Terakado M; Kurata H; Omi R; Kihara Y; Warshaviak D; Nakade S; Asmar-Rovira G; Mileni M; Mizuno H; Griffith MT; Rodgers C; Han GW; Velasquez J; Chun J; Stevens RC; Hanson MA Crystal structure of antagonist bound human lysophosphatidic acid receptor 1. Cell 2015, 161, 1633–1643. [PubMed: 26091040]

111. Hanson MA; Roth CB; Jo E; Griffith MT; Scott FL; Reinhart G; Desale H; Clemons B; Cahalan SM; Schuerer SC; Sanna MG; Han GW; Kuhn P; Rosen H; Stevens RC Crystal structure of a lipid G protein-coupled receptor. Science 2012, 335, 851–855. [PubMed: 22344443]

112. Yang YK; Dickinson CJ; Zeng Q; Li JY; Thompson DA; Gantz I Contribution of melanocortin receptor exoloops to Agouti-related protein binding. J Biol Chem 1999, 274, 14100–14106. [PubMed: 10318826]

113. Patel MP; Cribb Fabersunne CS; Yang YK; Kaelin CB; Barsh GS; Millhauser GL Loop-swapped chimeras of the agouti-related protein and the agouti signaling protein identify contacts required for melanocortin 1 receptor selectivity and antagonism. J Mol Biol 2010, 404, 45–55. [PubMed: 20831872]

114. Oosterom J; Garner KM; den Dekker WK; Nijenhuis WA; Gispen WH; Burbach JP; Barsh GS; Adan RA Common requirements for melanocortin-4 receptor selectivity of structurally unrelated melanocortin agonist and endogenous antagonist, Agouti protein. J Biol Chem 2001, 276, 931–936. [PubMed: 11024027]

115. Singh A; Haslach EM; Haskell-Luevano C Structure-activity relationships (SAR) of melanocortin and agouti-related (AGRP) peptides. Adv Exp Med Biol 2010, 681, 1–18. [PubMed: 21222256]

116. Joseph CG; Wang XS; Scott JW; Bauzo RM; Xiang Z; Richards NG; Haskell-Luevano C Stereochemical studies of the monocyclic agouti-related protein (103–122) Arg-Phe-Phe

residues: conversion of a melanocortin-4 receptor antagonist into an agonist and results in the discovery of a potent and selective melanocortin-1 agonist. J Med Chem 2004, 47, 6702–6710. [PubMed: 15615519]

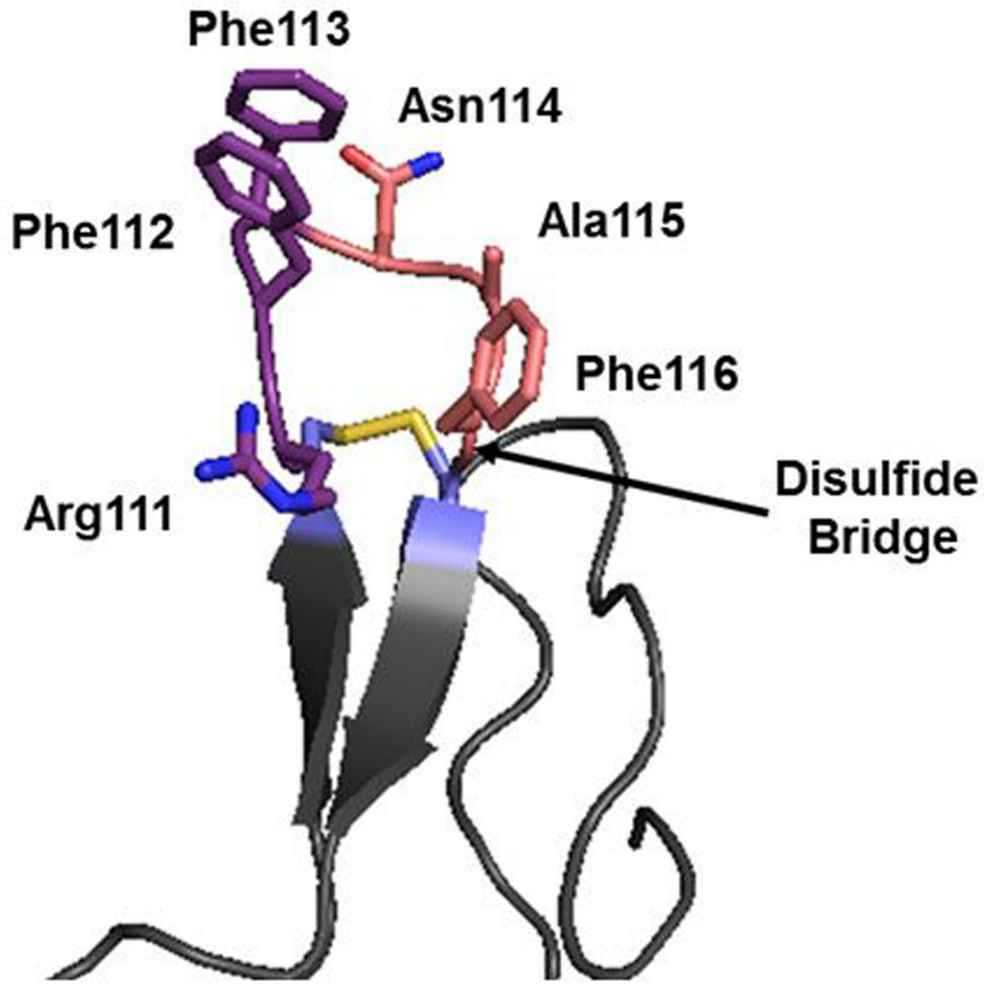


**Figure 1.**
Illustration of the proposed binding loop of AgRP, with the critical residues Arg-Phe-Phe in dark purple. PDB ID: 1HYK [72]

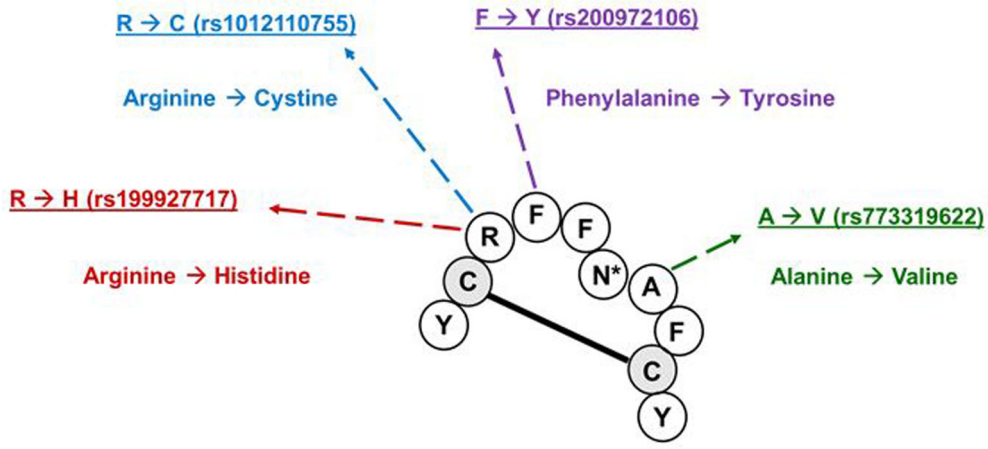


**Figure 2.**

SNPs in the purported binding loop of AgRP, deposited into the NIH Variation Viewer as of November 2017, (https://www.ncbi.nlm.nih.gov/variation/view/).

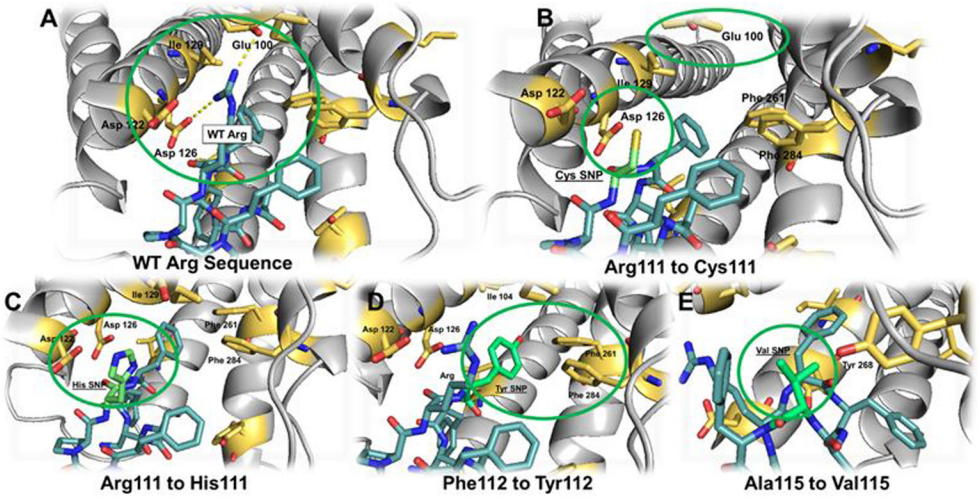


**Figure 3.**

Illustration of the Dap macrocyclic peptide scaffold containing the SNPs examined herein, docked into a GPCR homology molecular model of the human (hMC4R PDB ID:4z35-based model). SNPs are shown in green, while wild-type residues are shown in blue, interactions with hMC4R are shown in yellow, atom type is indicated with standard colors (O is red, N is blue, S is yellow). A) The wild-type Arg, with polar contacts shown in yellow dashes between Arg and Glu100/Asp126. B) The Arg to Cys SNP that possessed the greatest shift in potency. C) The His to Arg SNP containing peptide. D) The Phe to Tyr SNP containing peptide. E) The Ala to Val SNP containing peptide.

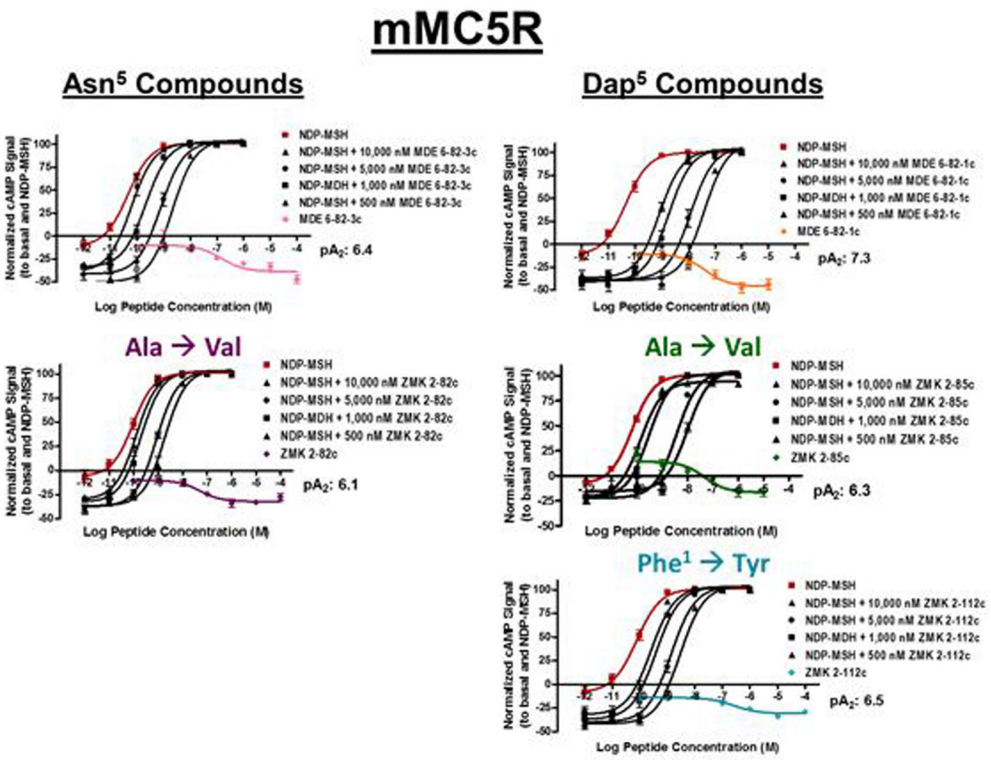


**Figure 4.**

Illustrations of the *in vitro* antagonist pharmacology of select orthosteric compounds at the mMC5R. The data has normalized to basal and NDP-MSH values in the cAMP accumulation assay. A Schild antagonist experimental design was applied and the agonist NDP-MSH was utilized in these experiments. Data points represent values from at least three independent experiments and the error bars represent the standard error of the mean (SEM).

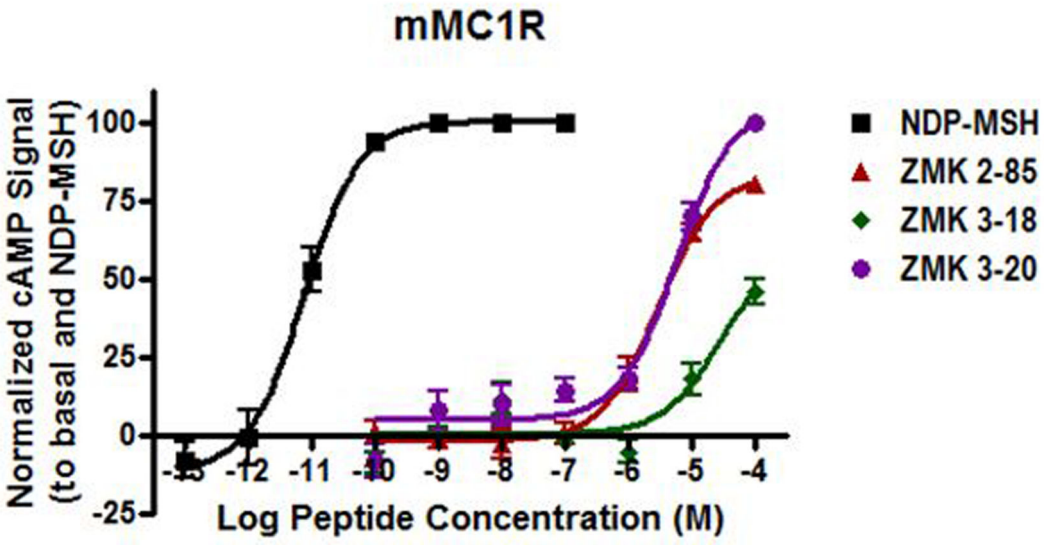


**Figure 5.**

Illustration of the agonist pharmacology observed for **ZMK2-85, ZMK3-18**, and **ZMK3-20** at the mMC1R, as compared to the control agonist NDP-MSH. Data points represent values from three independent experiments and error bars represent the standard error of the mean (SEM).

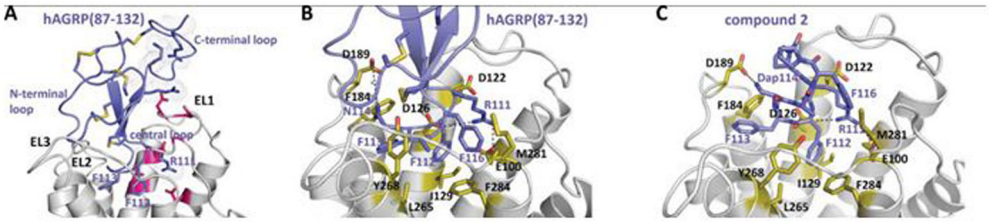


**Figure 6.**

Models of complexes of hMC4R (PDB ID: 4z35) with hAGRP(87-132) (A, B) and compound 2 (MDE 6-82-1c) octapeptide (C). (A) Ionic interactions between positively charged residues (shown by blue sticks with dots) from central and C-terminal loops of hAGRP(87-132) with patch of negatively charged residues (shown by red sticks) from TM2-EL1-TM3 of hMC4R; (B, C) Binging pocket residues of hMC4R (shown by yellow sticks with O-atoms colored red) that interacts with residues from central loop of AGRP (shown by blue sticks) in accordance with mutagenesis data [86, 112-114]. TM helices and extracellular loops (ELs) of hMC4R is shown by cartoons colored grey, ligands are shown by cartoon and sticks colored blue, five disulfide bridges in hAGRP are shown by blue sticks with S-atoms colored yellow.

**Table 1.**

Analytical data for peptides synthesized in this study.

| Peptide | Sequence | Retention Time (min)[a] | | M (calc) | mass spectral analysis (M+1) | Purity % |
|---|---|---|---|---|---|---|
| | | System 1 | System 2 | | | |
| **ZMK 2-82** | c[Pro-Arg-Phe-Phe-Asn-**Val**-Phe-DPro] | 19.5 | 31.1 | 1004.5 | 1005.6 | >98% |
| **ZMK 2-85** | c[Pro-Arg-Phe-Phe-*Dap*-**Val**-Phe-DPro] | 19.7 | 31.3 | 976.5 | 977.6 | >95% |
| **ZMK 2-96** | c[Pro-**His**-Phe-Phe-Asn-Ala-Phe-DPro] | 17.8 | 28.2 | 957.4 | 958.4 | >98% |
| **ZMK 2-99** | c[Pro-**His**-Phe-Phe-*Dap*-Ala-Phe-DPro] | 18.0 | 29.7 | 929.5 | 930.4 | >95% |
| **ZMK 2-110** | c[Pro-Arg-**Tyr**-Phe-Asn-Ala-Phe-DPro] | 15.4 | 24.6 | 992.5 | 993.5 | >99% |
| **ZMK 2-112** | c[Pro-Arg-**Tyr**-Phe-*Dap*-Ala-Phe-DPro] | 15.4 | 25.6 | 964.5 | 965.5 | >98% |
| **ZMK 3-18** | c[Pro-**Cys**-Phe-Phe-Asn-Ala-Phe-DPro] | 20.9 | 31.8 | 924.1 | 924.8 | >97% |
| **ZMK 3-20** | c[Pro-**Cys**-Phe-Phe-*Dap*-Ala-Phe-DPro] | 21.9 | 32.8 | 896.1 | 896.8 | >95% |

[a]Peptide retention times (min) are reported for solvent system 1 (10% acetonitrile in 0.1% trifluoroacetic acid/water and a gradient to 90% acetonitrile over 35 min) and solvent system 2 (10% methanol in 0.1% trifluoroacetic acid/water and a gradient to 90% methanol over 35 min). An analytical Vydac C18 column (Vydac 218TP104) was used with a flow rate of 1.5 mL/min. The peptide purity was determined by HPLC at a wavelength of 214 nm. Molecular mass was determined by MALDI-MS or ESI-TOF/MS (Applied Biosystems-Sciex 5800 MALDI/TOF/TOF-MS, Bruker BioTOF II ESI-TOF/MS, University of Minnesota Mass Spectrometry Lab).

**Table 2.**

Summary of the antagonist $pA_2$ and inverse agonist pharmacology of AgRP macrocyclic analogues incorporating both single nucleotide polymorphism mutations and Dap residues at the human melanocortin 4 receptor (hMC4R).[a]

| | Peptide | Sequence | hMC4R $pA_2$ | Observed Inverse Agonism? |
|---|---|---|---|---|
| | **AgRP** | | 8.7 ± 0.1 | Yes |
| | **1*** **(MDE 6-82-3c)** | c[Pro-Arg-Phe-Phe-Asn-Ala-Phe-DPro] | 8.0 ± 0.2 | Yes |
| | **ZMK 2-82** | c[Pro-Arg-Phe-Phe-Asn-**Val**-Phe-DPro] | 7.8 ± 0.03 | Yes |
| **ASN** [5] | **ZMK 2-96** | c[Pro-**His**-Phe-Phe-Asn-Ala-Phe-DPro] | 5.8 ± 0.2 | Yes |
| | **ZMK 2-110** | c[Pro-Arg-**Tyr**-Phe-Asn-Ala-Phe-DPro] | 6.5 ± 0.2 | Yes |
| | **ZMK 3-18** | c[Pro-**Cys**-Phe-Phe-Asn-Ala-Phe-DPro] | 5.8 ± 0.2 | No |
| | **2*** **(MDE 6-82-1c)** | c[Pro-Arg-Phe-Phe-*Dap*-Ala-Phe-DPro] | 8.6 ± 0.2 | Yes |
| | **ZMK 2-85** | c[Pro-Arg-Phe-Phe-*Dap*-**Val**-Phe-DPro] | 7.6 ± 0.06 | Yes |
| **DAP** [5] | **ZMK 2-99** | c[Pro-**His**-Phe-Phe-*Dap*-Ala-Phe-DPro] | 6.4 ± 0.09 | No |
| | **ZMK 2-112** | c[Pro-Arg-**Tyr**-Phe-*Dap*-Ala-Phe-DPro] | 7.5 ± 0.2 | Yes |
| | **ZMK 3-20** | c[Pro-**Cys**-Phe-Phe-*Dap*-Ala-Phe-DPro] | <5.0 | No |

[a]The indicated errors represent the standard error of the mean (SEM) determined from at least three independent experiments. The antagonistic $pA_2$ values were determined using the Schild analysis and the agonist NDP-MSH. >100,000 indicates that the compound was examined but lacked agonist activity at up to 100 μM concentrations. <5.0 indicates that no antagonist potency was observed in the highest concentration ranged assayed (10,000, 5,000, 1,000, and 500 nM). Inverse agonist indicates that inverse agonist pharmacology was observed.

*The pharmacology for **1** and **2** has previously been reported.[80]

**Table 3.**

Summary of the cAMP based agonist $EC_{50}$ and antagonist $pA_2$ pharmacology values of AgRP macrocyclic analogues incorporating both single nucleotide polymorphism mutations and Dap residues at the mouse melanocortin receptors.[a]

| | Peptide | Sequence | mMC1R | mMC3R | | mMC4R | | mMC5R | |
|---|---|---|---|---|---|---|---|---|---|
| | | | $EC_{50}$ (nM) | $EC_{50}$ (nM) | $pA_2$ | $EC_{50}$ (nM) | $pA_2$ | $EC_{50}$ (nM) | $pA_2$ |
| | NDP-MSH | | 0.010±0.003 | 0.07±0.03 | | 0.9±0.6 | | 0.13±0.03 | |
| **ASN** [5] | **1*** **(MDE 6-82-3c)** | c[Pro-Arg-Phe-Phe-Asn-Ala-Phe-DPro] | 25% @ 100 μM | >100,000 | 6.3 ± 0.1 | >100,000 | 8.2 ± 0.1 | Inverse Agonist −10% | 6.4 ± 0.2 |
| | **ZMK 2-82** | c[Pro-Arg-Phe-Phe-Asn-**Val**-Phe-DPro] | 23% @ 100 μM | >100,000 | 5.9 ± 0.1 | 16% @ 100 μM | 7.2 ± 0.1 | >100,000 | 6.1 ± 0.09 |
| | **ZMK 2-96** | c[Pro-**His**-Phe-Phe-Asn-Ala-Phe-DPro] | 23% @ 100 μM | >100,000 | < 5.0 | >100,000 | 5.3 ± 0.1 | >100,000 | N/A |
| | **ZMK 2-110** | c[Pro-Arg-**Tyr**-Phe-Asn-Ala-Phe-DPro] | >100,000 | >100,000 | 5.8 ± 0.2 | >100,000 | 6.1 ± 0.03 | Inverse Agonist −35% @ 100 μM | N/A |
| | **ZMK 3-18** | c[Pro-**Cys**-Phe-Phe-Asn-Ala-Phe-DPro] | 46% @ 100 μM | >100,000 | < 5.0 | >100,000 | 5.9 ± 0.1 | Inverse Agonist −32% @ 100 μM | <5.0 |
| **DAP** [5] | **2*** **(MDE 6-82-1c)** | c[Pro-Arg-Phe-Phe-*Dap*-Ala-Phe-DPro] | 30% @ 100 μM | >100,000 | 6.5 ± 0.09 | >100,000 | 8.7 ± 0.1 | Inverse Agonist −15% | 7.3 ± 0.03 |
| | **ZMK 2-85** | c[Pro-Arg-Phe-Phe-*Dap*-**Val**-Phe-DPro] | 79% @ 100 μM | 27% @ 100 μM | 6.1± 0.03 | 37% @ 100 μM | 7.5 ± 0.1 | >100,000 | 6.3 ± 0.03 |
| | **ZMK 2-99** | c[Pro-**His**-Phe-Phe-*Dap*-Ala-Phe-DPro] | 56% @ 100 μM | >100,000 | 5.4 ± 0.1 | >100,000 | 6.0 ± 0.1 | >100,000 | N/A |
| | **ZMK 2-112** | c[Pro-Arg-**Tyr**-Phe-*Dap*-Ala-Phe-DPro] | 48% @ 100 μM | >100,000 | 6.5 ± 0.1 | >100,000 | 7.3 ± 0.1 | >100,000 | 6.5 ± 0.2 |
| | **ZMK 3-20** | c[Pro-**Cys**-Phe-Phe-*Dap*-Ala-Phe-DPro] | 4000 ± 2000 | 29% @ 100 μM | < 5.0 | 42% @ 100 μM | < 5.0 | >100,000 | N/A |

[a]The indicated errors represent the standard error of the mean (SEM) determined from at least three independent experiments. The antagonistic $pA_2$ values were determined using the Schild analysis and the agonist NDP-MSH. >100,000 indicates that the compound was examined but lacked agonist activity at up to 100 μM concentrations. N/A indicates that the compound was not examined. A percentage denotes the percent maximal stimulatory response observed at 100 μM concentrations but not enough stimulation was observed to determine an $EC_{50}$ value. <5.0 indicates that no antagonist potency was observed in the highest concentration ranged assayed (10,000, 5,000, 1,000, and 500 nM). Inverse agonist indicates that inverse agonist pharmacology was observed with the percent decrease from basal indicated. For inverse agonists, a decrease in cAMP signal was observed without a sigmoidal dose-response curve, the percent change from basal at 100 μM concentrations is indicated.

*The pharmacology for **1** and **2** has previously been reported, with the exception of the antagonistic $pA_2$ values at the mMC5R which are reported herein for the first time.

*J Med Chem*. Author manuscript; available in PMC 2021 March 12.

**Table 4.**

Summary of binding $IC_{50}$ affinities using the $^{125}$I-NDP-MSH orthosteric binding ligand, of AgRP macrocyclic analogues incorporating both single nucleotide polymorphism mutations and Dap residues at the mouse melanocortin receptors (mMCRs).[a]

| | Peptide | Sequence | mMC1R | | mMC3R | | mMC4R | | mMC5R | |
|---|---|---|---|---|---|---|---|---|---|---|
| | | | $IC_{50}$ (nM) | Fold Diff | $IC_{50}$ (nM) | Fold Diff | $IC_{50}$ (nM) | Fold Diff | $IC_{50}$ (nM) | Fold Diff |
| | NDP-MSH | | 0.29 ± 0.09 | | 8.2 ± 0.7 | | 1.30 ± 0.01 | | 140 ± 50 | |
| **ASN** [5] | **1 (MDE 6-82-3c)** | c[Pro-Arg-Phe-Phe-Asn-Ala-Phe-DPro] | 9000 ± 2000 | **1** | 17000 ±5500 | **1** | 70 ± 20 | **1** | 12300 ± 800 | **1** |
| | **ZMK 2-82** | c[Pro-Arg-Phe-Phe-Asn-**Val**-Phe-DPro] | 15000 ± 8000 | 2 | 53000 ± 11000 | 3 | 38 ± 2 | 2 | 29000 ±3000 | 2 |
| | **ZMK 2-96** | c[Pro-**His**-Phe-Phe-Asn-Ala-Phe-DPro] | >100,000 | | >100,000 | | 6700 ± 600 | 300 | >100,000 | |
| | **ZMK 2-110** | c[Pro-Arg-**Tyr**-Phe-Asn-Ala-Phe-DPro] | >100,000 | | >100,000 | | 2000 ± 100 | 100 | >100,000 | |
| | **ZMK 3-18** | c[Pro-**Cys**-Phe-Phe-Asn-Ala-Phe-DPro] | 24600 ± 100 | 3 | >100,000 | | 1900 ± 500 | 90 | >100,000 | |
| **DAP** [5] | **2 (MDE 6-82-1c)** | c[Pro-Arg-Phe-Phe-*Dap*-Ala-Phe-DPro] | 5200 ± 300 | **1** | 3200 ± 600 | **1** | 1.9 ± 0.6 | **1** | 1700 ± 300 | **1** |
| | **ZMK 2-85** | c[Pro-Arg-Phe-Phe-*Dap*-**Val**-Phe-DPro] | 8000 ± 5000 | 2 | 10000 ± 100 | 3 | 8.2 ± 0.8 | 4 | 2700 ± 100 | 2 |
| | **ZMK 2-99** | c[Pro-**His**-Phe-Phe-*Dap*-Ala-Phe-DPro] | 25000 ± 6000 | 5 | 15000 ± 3000 | 5 | 1000 ± 300 | 500 | 12000 ± 6000 | 7 |
| | **ZMK 2-112** | c[Pro-Arg-**Tyr**-Phe-*Dap*-Ala-Phe-DPro] | 18000 ± 1000 | 4 | 28000 ± 12000 | 9 | 134 ± 7 | 70 | 36000 ± 2000 | 20 |
| | **ZMK 3-20** | c[Pro-**Cys**-Phe-Phe-*Dap*-Ala-Phe-DPro] | 33000 ± 2000 | 6 | 49000 ± 3000 | 15 | 10000 ± 2000 | 5200 | >100,000 | |

[a]The indicated errors represent the standard deviation (SD) determined from at least two independent experiments, each consisting of duplicate replicates. >100,000 indicates that the compound was examined but lacked binding affinity at up to 100 μM concentrations. In addition, NDP-MSH, c[Pro-Arg-Phe-Phe-Asn-Ala-Phe-DPro], and c[Pro-Arg-Phe-Phe-*Dap*-Ala-Phe-DPro] are included as experimental controls and as reference controls. The fold difference (fold diff) is determined between the peptide as compared to the c[Pro-Arg-Phe-Phe-Asn-Ala-Phe-DPro] or c[Pro-Arg-Phe-Phe-*Dap*-Ala-Phe-DPro] controls respectively.

**Table 5.**

Summary of binding affinity $IC_{50}$ values using the $^{125}$I-NDP-MSH orthosteric agonist ligand to competitively displace the AgRP based macrocyclic analogues incorporating both single nucleotide polymorphism mutations and Dap residues at the hMC4R.[a]

| | Peptide | Sequence | hMC4R | |
|---|---|---|---|---|
| | | | $IC_{50}$ (nM) | Fold Diff |
| | NDP-MSH | | 10 ± 2 | |
| **ASN** [5] | **1 (MDE 6-82-3c)** | c[Pro-Arg-Phe-Phe-Asn-Ala-Phe-DPro] | 70 ± 20 | 1 |
| | **ZMK 2-82** | c[Pro-Arg-Phe-Phe-Asn-**Val**-Phe-DPro] | 250 ± 40 | 3 |
| | **ZMK 2-96** | c[Pro-**His**-Phe-Phe-Asn-Ala-Phe-DPro] | 22000 ± 2000 | 300 |
| | **ZMK 2-110** | c[Pro-Arg-**Tyr**-Phe-Asn-Ala-Phe-DPro] | 14300 ± 1200 | 2000 |
| | **ZMK 3-18** | c[Pro-**Cys**-Phe-Phe-Asn-Ala-Phe-DPro] | 19300 ± 1400 | 300 |
| **DAP** [5] | **2 (MDE 6-82-1c)** | c[Pro-Arg-Phe-Phe-*Dap*-Ala-Phe-DPro] | 7.5 ± 0.4 | 1 |
| | **ZMK 2-85** | c[Pro-Arg-Phe-Phe-*Dap*-**Val**-Phe-DPro] | 32.2 ± 0.5 | 4 |
| | **ZMK 2-99** | c[Pro-**His**-Phe-Phe-*Dap*-Ala-Phe-DPro] | 2700 ± 600 | 400 |
| | **ZMK 2-112** | c[Pro-Arg-**Tyr**-Phe-*Dap*-Ala-Phe-DPro] | 1016 ± 9 | 100 |
| | **ZMK 3-20** | c[Pro-**Cys**-Phe-Phe-*Dap*-Ala-Phe-DPro] | 15700 ± 1400 | 2100 |

[a]The indicated errors represent the standard deviation determined from at least two independent experiments, each consisting of duplicate replicates. >100,000 indicates that the compound was examined but lacked binding affinity at up to 100 μM concentrations. NDP-MSH, c[Pro-Arg-Phe-Phe-Asn-Ala-Phe-DPro], and c[Pro-Arg-Phe-Phe-*Dap*-Ala-Phe-DPro] are included as experimental controls and reference controls. The fold difference (fold diff) is determined between the peptide as compared to the c[Pro-Arg-Phe-Phe-Asn-Ala-Phe-DPro] or c[Pro-Arg-Phe-Phe-*Dap*-Ala-Phe-DPro] controls respectively.